

SFQED Processes at ELI-NP

M. Pentiã – Sesiune Științifică Fac. Fizică 2023

1. Light – Matter interaction processes

The simplest QED interaction processes between light and matter possible to be measured at ELI-NP Facility. Feynman diagrams evaluations.

Fundamental Interactions : Light & Matter

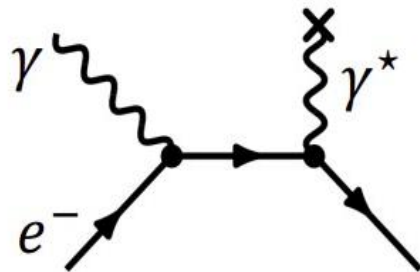
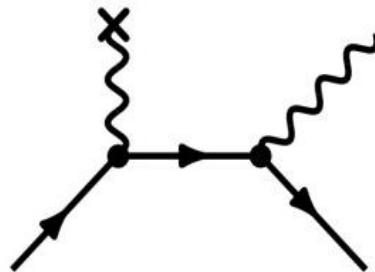
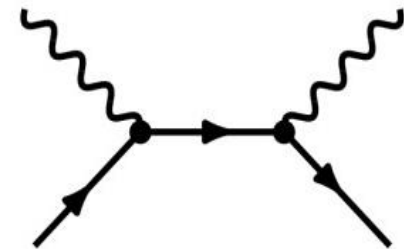


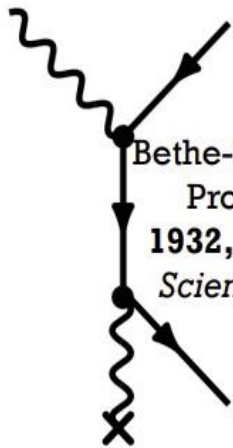
Photo Electric Effect
1887 Hertz, *Ann Phys*
(*Leipzig*) 31, 983



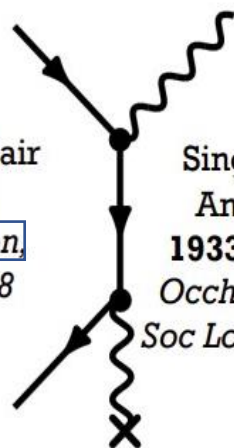
Bremsstrahlung
1895 Röntgen, *Ann Phys*
(*Leipzig*) 300, 1



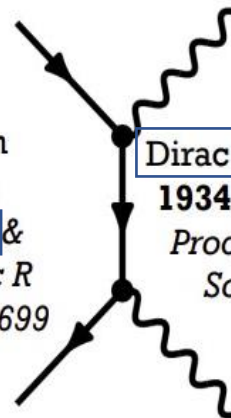
Compton Scattering
1906 Thomson, *Conduction of*
Electricity through Gases



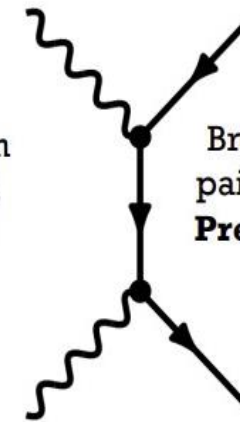
Bethe-Heitler Pair
Production
1932, Anderson,
Science 76,238



Single Photon
Annihilation
1933, Blackett &
Occhialini, *Proc R*
Soc Lond A 139, 699



Dirac Annihilation
1934, Klempner,
Proc Camb Phil
Soc 30, 347

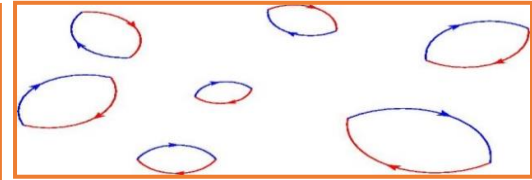


Breit-Wheeler
pair production
Predicted 1934

$$E_{\min}^* > 2 \cdot 0.511 \text{ MeV}$$

1. Vacuum local fluctuation - Schwinger field E_{cr}

Under normal conditions, the physical vacuum, due to the quantum fluctuations, is in a permanent "boiling", with local production and annihilation of *virtual* particle-antiparticle pairs.



According to the Heisenberg principle, locally, on short time intervals Δt , there are energy fluctuations ΔE , so their product cannot be smaller than \hbar .

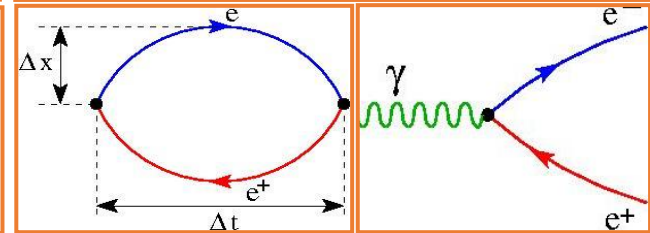
$$\Delta E \cdot \Delta t \geq \hbar$$

$$\begin{aligned} \hbar &= 1.054571817 \times 10^{-34} \text{ J} \cdot \text{s} \\ &= 6.582119569 \times 10^{-16} \text{ eV} \cdot \text{s} \end{aligned}$$

Then, on Δt time intervals, we have ΔE energy fluctuations that allow production of e^+e^- pairs:

$$\begin{aligned} \Delta E &\approx 2 m_e c^2 = 2 \cdot 0.511 \text{ MeV} \approx 10^6 \text{ eV} \\ \Delta t &\geq \hbar / 2m_e c^2 = 10^{-22} \text{ s} \end{aligned}$$

Locally on Δx space can be produced electron-positron pairs, which live on the average Δt time, then they annihilate. A strong electric field can transfer enough energy to transform virtual pairs into real pairs.



The characteristic range $2\Delta x$ the electric field can produce e^+e^- pairs is given by *electron reduced Compton wavelength*

$$2\Delta x \approx 2c\Delta t = \frac{\hbar}{m_e c} = \tilde{\lambda}_c \approx 386 \cdot 10^{-15} \text{ m}$$

The virtual e^+e^- pair becomes a real one if a minimum energy W is transferred by the electric field E

$$W = F \cdot \tilde{\lambda} = \frac{eE\hbar}{m_e c} > 2m_e c^2$$

or minimum value of the electric field is

$$E > \frac{2m_e^2 c^3}{\hbar e} = 2E_{cr}$$

The critical value of the electric field E_{cr} (*Schwinger field*) i.e. starting value for spontaneously production of real e^+e^- pairs from laser field - vacuum interaction:

$$E_{cr} = \frac{m_e^2 c^3}{\hbar e} = 1.323 \cdot 10^{18} \text{ V / m}$$

1. Conversion of Light to Matter

One of the fundamental electromagnetic interaction processes, little studied experimentally, is the **conversion of light to matter**.

Particle production from the e.m. field, one of the amazing predictions of the QED, is possible, at least in principle, in connection with the vacuum particle pair production:

➤ in a static electric field – **Schwinger effect** [1]

➤ in a photon field – **Breit-Wheeler production** [2-5]

$$\gamma + \gamma \rightarrow e^+ + e^- \quad \text{or} \quad \gamma + n\gamma \rightarrow e^+ + e^-$$

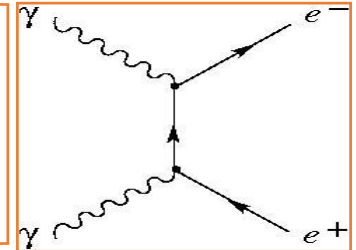
➤ in a combination of the two – **Bethe-Heitler production** [6]

$$n\gamma_R + \gamma_V \rightarrow e^+ + e^-$$

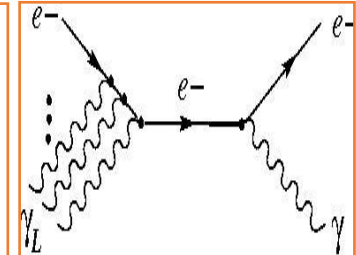
1. QED Processes - Conversion of Light to Matter

So far, the current theoretical and experimental works with high-power lasers have highlighted a series of QED processes and confirmed the possibility to approach them experimentally.

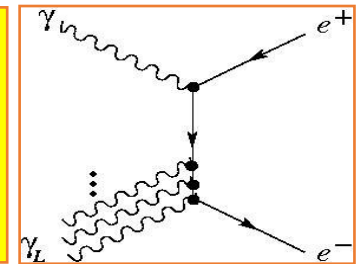
- **The linear Breit-Wheeler (BW) process** [2] $\gamma + \gamma \rightarrow e^- + e^+$ has been studied in the the framework of QED [24]. To date, the linear BW process has not been observed in the laboratory with **real photons** due to the lack of suitably bright sources of photons with sufficient energy.



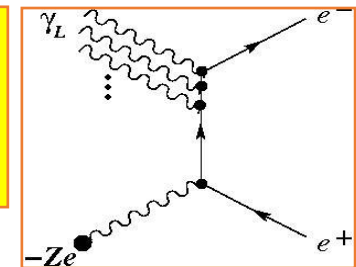
- **Nonlinear (multiphoton) inverse Compton scattering** $e^- + n \gamma_L \rightarrow e^- + \gamma$ where the electron, e^- , absorbs multiple, n laser photons γ_L , and radiates hard photons γ . Up to 40% of the energy of the laser accelerated electrons is re-radiated as gamma photons in the presence of the laser field [26]



- **Nonlinear (multiphoton) Breit-Wheeler process:** $\gamma + n \gamma_L \rightarrow e^- + e^+$ where the electron - positron pair is generated. Hence for the energy of multiple laser photons, pure energy is transformed into the mass of the particles: electrons and positrons. Light is transformed into matter [27]



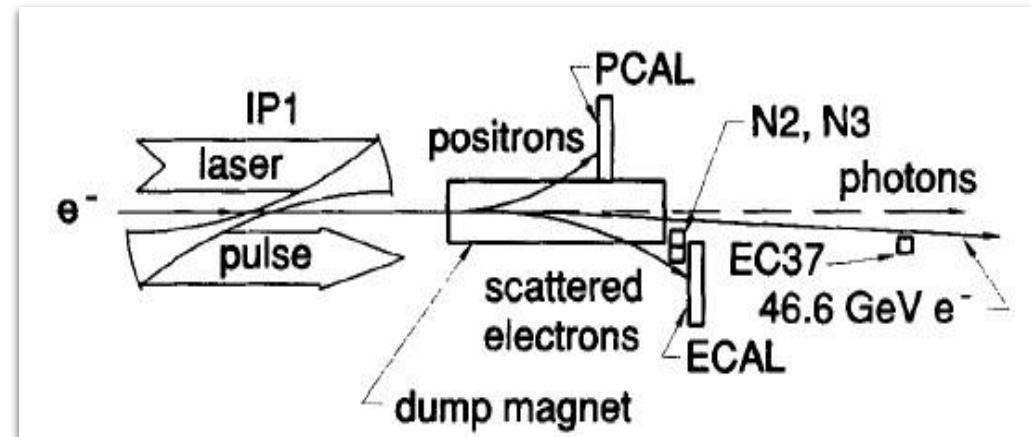
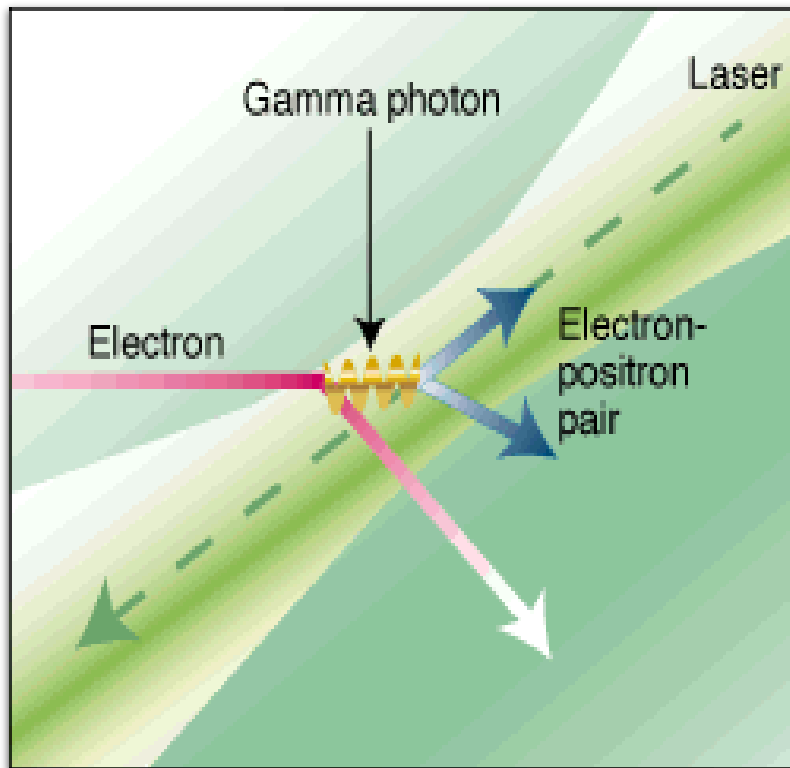
- **Bethe-Heitler (BH) interaction process with nuclei** [28] $n \gamma_L + \gamma_V \rightarrow e^- + e^+$ where the multiple laser photons in interaction with the **virtual photon** of the nucleus field, transfer energy to $e^+ e^-$ production process.



E-144 SLAC Experiment (electron – laser collision) - 1997

In this experiment [14] 46.6 GeV electrons were scattered in the terawatt laser strong e.m. field. Infrared laser radiation of wavelength 527 nm (2.35 eV), pulses of 650 mJ , intensity 10^{18} W/cm^2 were used.

Parameters of the experiment correspond to the regime of nonlinear Compton scattering.



E-144 SLAC Experiment

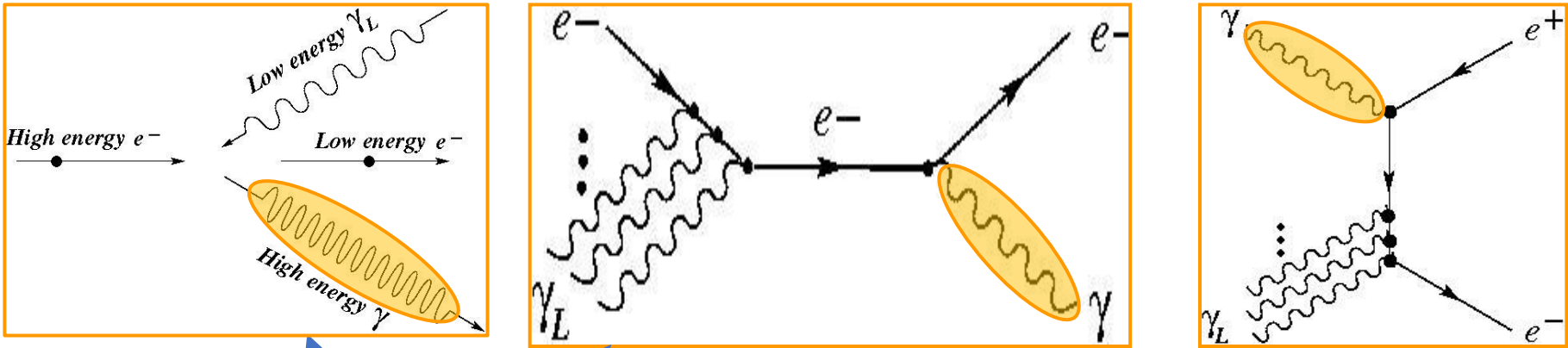
$$\gamma + n \gamma_0 \rightarrow e^+ e^-$$

106 ± 14 positrons observed:

P.R.L. 79, 1626 (1997) [14]

E-144 SLAC Experiment (electron – laser collision) - 1997

E-144 Collaboration, <https://doi.org/10.1063/1.52962>



For production of an electron-positron pair, the center-of-mass energy of the scattering photons must be at least $2mc^2 \sim 1 \text{ MeV}$.

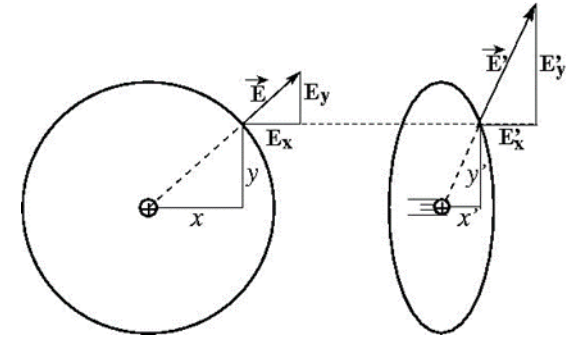
This can be achieved by scattering a laser beam against a high-energy photon beam created, for example, by backscattering the laser beam off a high-energy electron beam.

With laser light of wavelength 527 nm (energy 2.35 eV), would be required a photon of energy 109 GeV for reaction $\gamma_1 \gamma_2 \rightarrow e^+ e^-$ to proceed.

However, with an electron beam of energy 46.6 GeV as available at the Stanford Linear Accelerator Center (SLAC) the maximum Compton-backscattered photon energy from a 527 nm laser is only 29.2 GeV .

How can explain SLAC results ?

- The **SLAC experiment E-144** for the first time measured **nonlinear Compton scattering and pair production** in the **interaction of a high energy electron beam with an intense laser in the multi-photon regime** ($n > 4$) [13, 14].
- When a laser electric field of strength E_L in the rest frame of a relativistic, counter-propagating electron with laboratory energy E_e and Lorentz factor $\gamma_e = \mathcal{E}_e / mc^2 \gg 1$ the **laser electric field strength appears boosted** to $E^* = 2\gamma_e E_L$

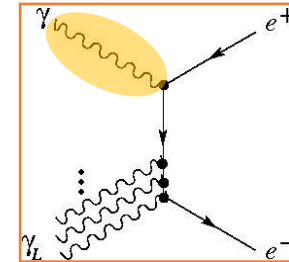
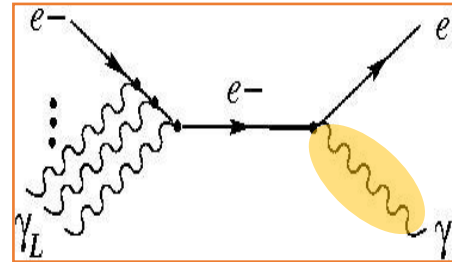
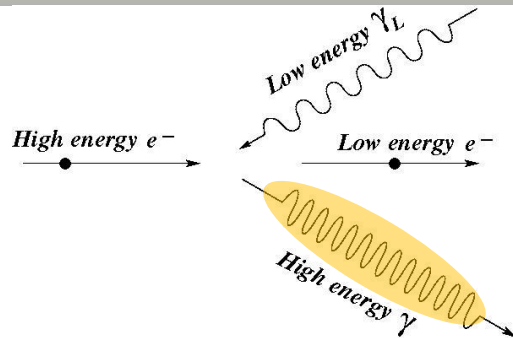


For $\mathcal{E}_e = 46.6 \text{ GeV}$ electron has $\gamma_e = 46.6 \times 10^3 \text{ MeV} / 0.511 \text{ MeV} = 9 \times 10^4$ so if it collides head on with a 527 nm laser pulse of strength $\xi = 1$ the field in the electron's rest frame is $E^* = 1.1 \times 10^{18} \text{ V/m}$.

This is close to the QED critical strength $E_{cr} = m^2 c^3 / \hbar e = 1.3 \times 10^{18} \text{ V/m}$ at which the energy gain of an electron accelerating over a Compton wavelength is its rest energy, and at which a static electric field would spontaneously break down into electron-positron pairs.

E-144 SLAC Experiment (electron – laser collision) - 1997

(Skip)



When an ultra-relativistic electron (from a beam) of initial energy $\varepsilon_0 \gg mc^2$ absorbs n photons, each of energy $\hbar\omega \ll mc^2$, from a laser pulse that crosses the electron beam at the angle θ_0 , the minimum energy of the scattered electron is

$$\varepsilon_{\min} = \frac{\varepsilon_0}{1 + \left(2n\varepsilon_0\omega_0 / m_*^2 c^4\right) (1 + \cos \theta_0)}$$

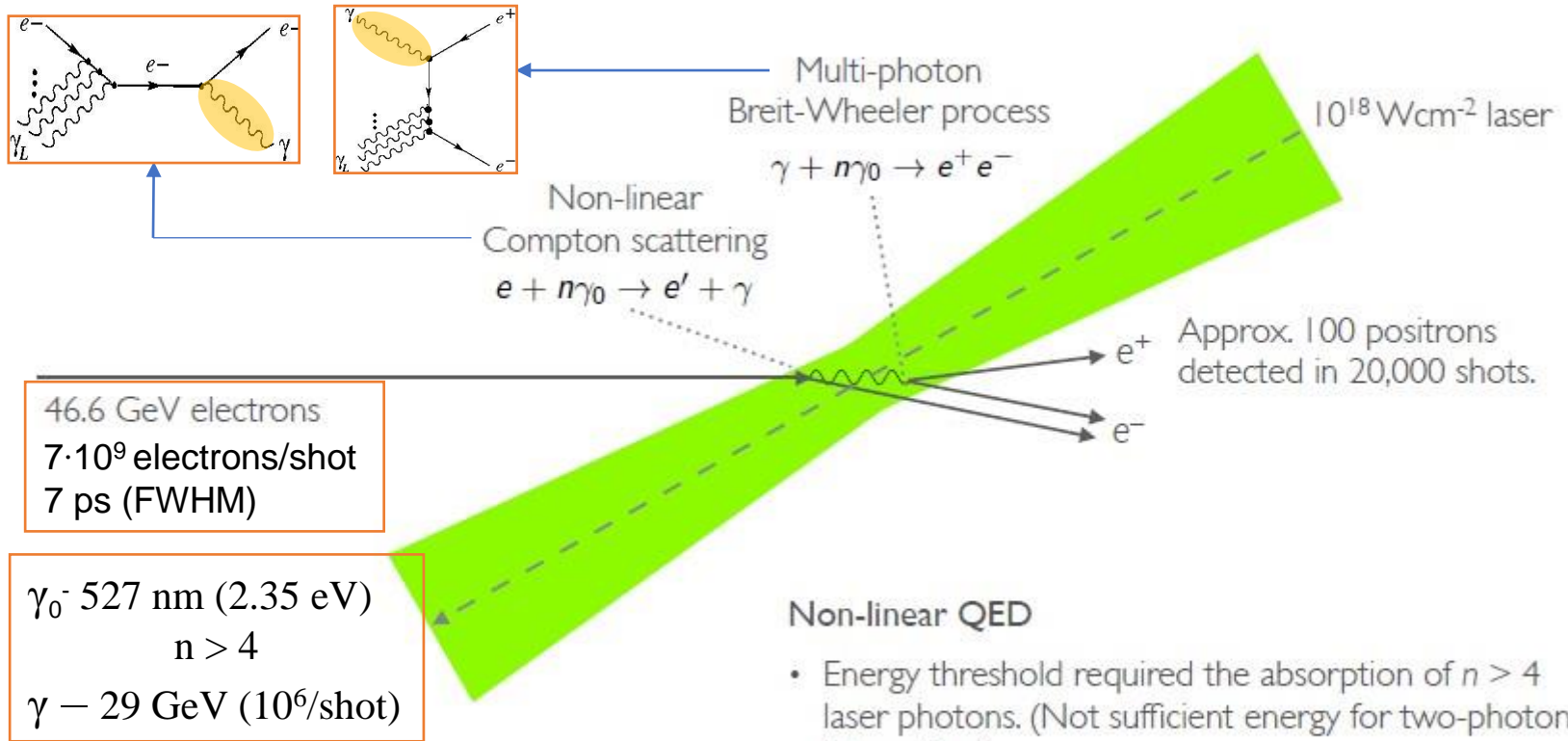
where $m_* = m\sqrt{1 + q^2 / 2}$ is the effective mass (Volkov states) of the electron in the laser field of linear polarization and frequency ω_0 and for laser field strength $q = eA_0 / mc^2$

We see that the minimum energy in the **scattered electron spectrum depends on the number of photons absorbed from the laser field and, therefore, can serve as a signature of the nonlinear Compton effect.**

For linear Compton scattering ($n = 1$) one obtains the scattered electron minimum energy $\varepsilon_{\min} = 25.6 \text{ GeV}$, using parameters from the experiment ($\varepsilon_0 = 46.6 \text{ GeV}$, $\theta_0 = 17^\circ$, and $\lambda = 1054 \text{ nm}$). But, for the two- and three-photon (nonlinear Compton effect) the electron spectrum threshold is found to be at 17.6 and 13.5 GeV, respectively.

E-144 SLAC Experiment (electron – laser collision) - 1997

SLAC E-144 experiment:
first sign of positron production in light-by-light scattering



46.6 GeV electrons
 $7 \cdot 10^9$ electrons/shot
7 ps (FWHM)

γ_0 : 527 nm (2.35 eV)
 $n > 4$
 γ – 29 GeV (10^6 /shot)

Non-linear QED

- Energy threshold required the absorption of $n > 4$ laser photons. (Not sufficient energy for two-photon interaction.)
- Recently shown that, on average, $n = 6.44$ laser photons were absorbed.

Burke et al., PRL 79, 1626 (1997)
Hu & Müller, PRL 107, 090402 (2010)

2. ELI QED History

Dream 2009

In 2009 G. V. Dunne (University of Connecticut) in the paper “New strong-field QED effects at extreme light infrastructure” in Eur. Phys. J. D 55, 327–340 (2009) remarked “**the ELI project open up an entirely new non-perturbative regime of QED**, and of quantum field theories in general. **There are many experimental and theoretical challenges ahead**. Theoretically, the biggest challenge in the non-perturbative arena is to develop efficient techniques, both analytical and numerical, for computing the effective action and related quantities, in external fields that realistically represent the experimental laser configurations. A lot of progress has been made in this direction, but new ideas and methods are still needed”.

On the other hand, production of large numbers of MeV positrons in the laboratory opens the door to new avenues of antimatter research, including an understanding the physics of various astrophysical phenomena such as black holes and gamma ray bursts [45,46], pair plasma physics [47,48] and positronium production.

Today 2023

Now the 2 x 10 PW laser beams of the ELI-NP laser facility has the interaction chambers dedicated to QED experiments [42-44]. So, we can move on to fruition this possibility **to in-depth study of nonlinear QED processes** with such laser beams to perform the following steps:

- Systematic studies of the dynamics of fundamental QED processes possible to approach with high power lasers, in order to reveal characteristic properties of the processes as: **Breit-Wheeler e^+e^- pair production, Bethe-Heitler e^+e^- pair production, Dirac e^+e^- pair annihilation, e^-e^- Moller Scattering, e^-e^+ Bhabha Scattering, Electron Self Energy, Photon Self Energy, Vacuum Energy.**
- Proposal of experimental works for measuring physical properties related to the production of e^+e^- pairs (Schwinger mechanism) in photon-multiphoton interaction (Breit-Wheeler), photon-electron or photon-nucleus (Bethe-Heitler) interaction and production and measurement of QED bound states (positronium).

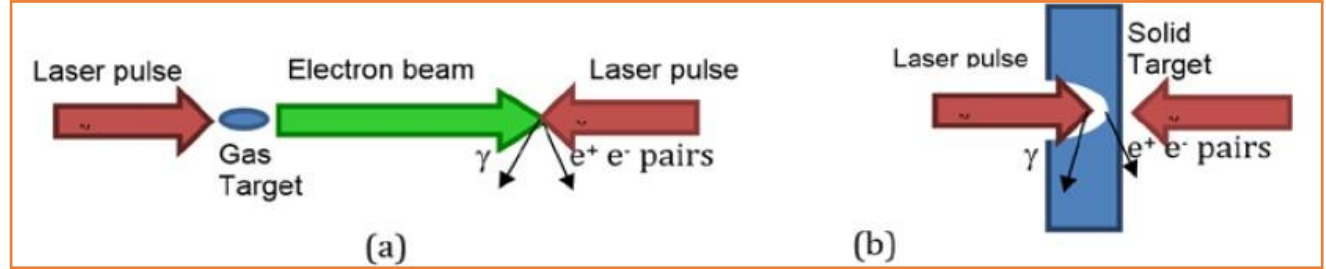
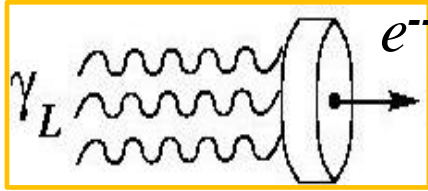
(conditioned by adequate funding for manpower, equipment and materials).

Tomorrow

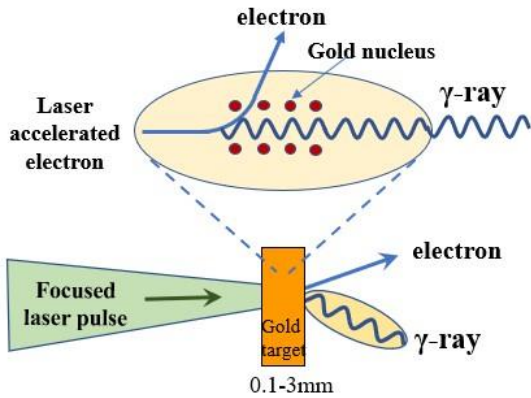
Experimental measurement of some fundamental QED processes with High Power Lasers at ELI-NP.

2. Particular interest - multiphoton Breit-Wheeler pair production

Wakefield acceleration

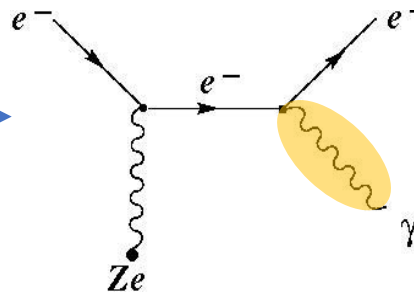


Bremsstrahlung



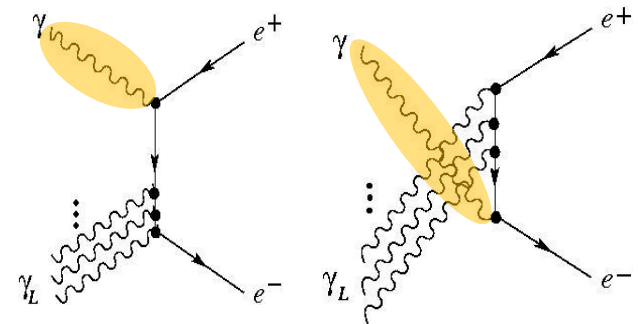
MeV γ sources

Bremsstrahlung

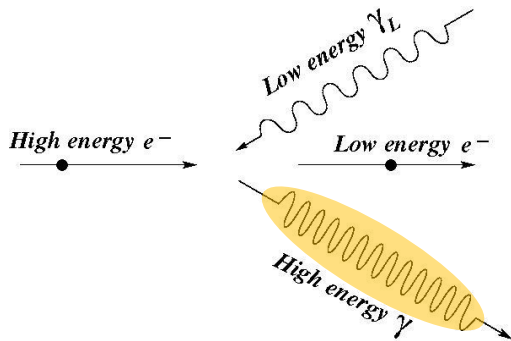


Pair production

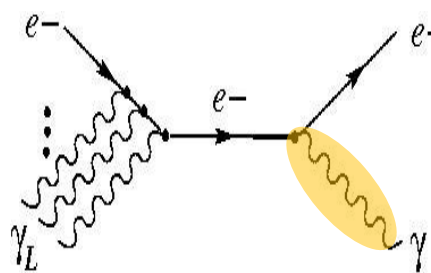
Breit-Wheeler pair production



Inverse Compton scattering

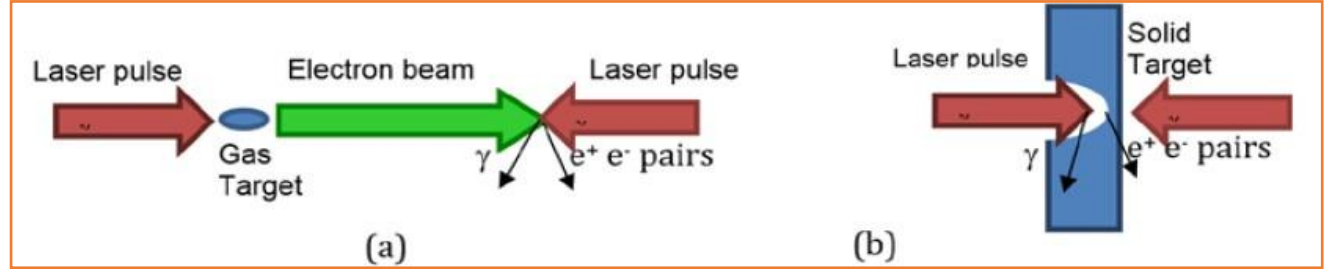
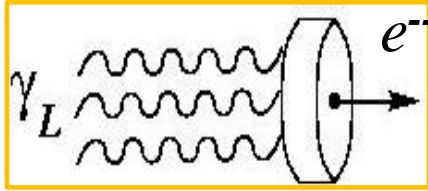


Inverse Compton scattering

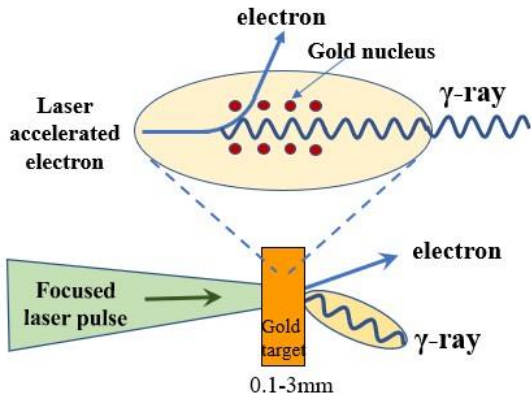


2. Particular interest - multiphoton Bethe-Heitler pair production

Wakefield acceleration

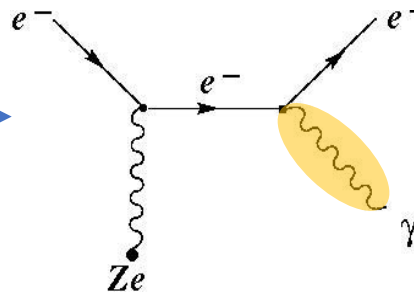


Bremsstrahlung



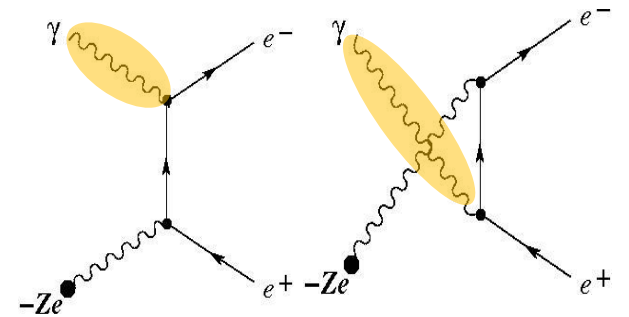
MeV γ sources

Bremsstrahlung

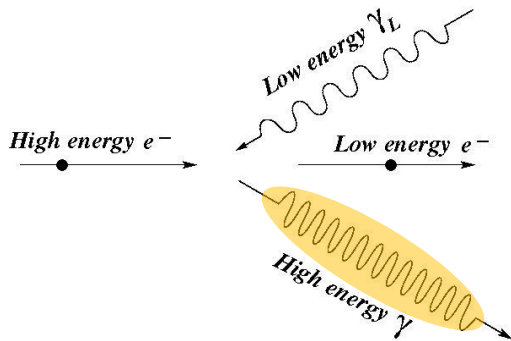


Pair production

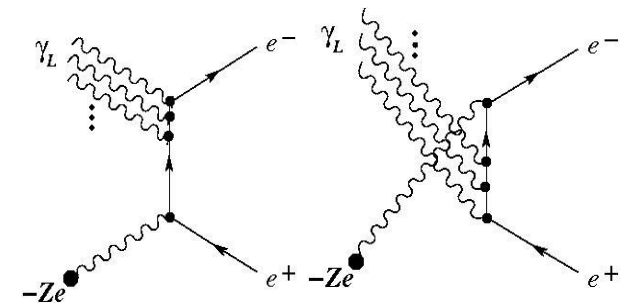
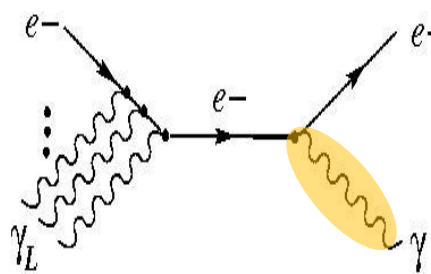
Bethe-Heitler pair production



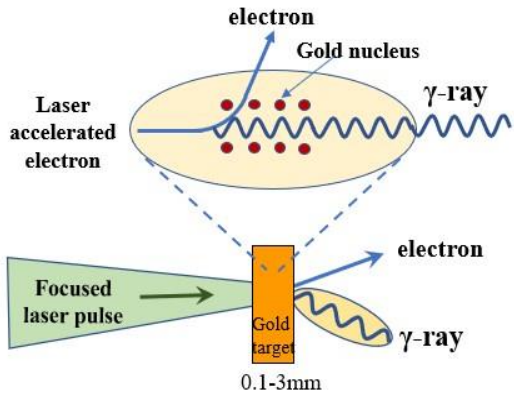
Inverse Compton scattering



Inverse Compton scattering

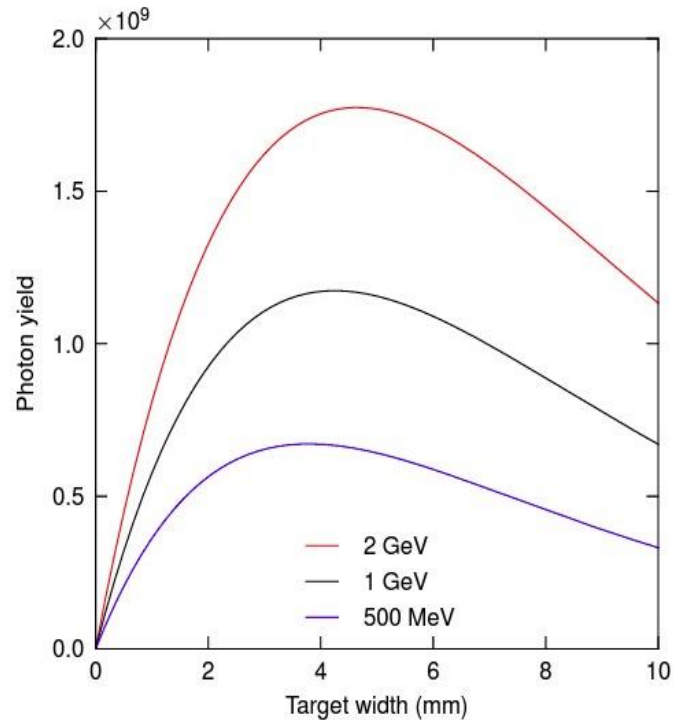


2. γ -ray production by electron bremsstrahlung



High conversion of electrons into gamma-rays can be achieved using bremsstrahlung in a gold target

Number of photons emitted over 100 MeV



- Ultra-relativistic electrons lose energy in gold almost solely by bremsstrahlung. (Other loss mechanisms such as ionisation and Compton scattering are suppressed at GeV energies.)
- Cross-section well known:

$$\frac{d\sigma_{eZ}}{d\omega}(\omega, y) = \frac{\alpha r_0^2}{\omega} \left\{ \left(\frac{4}{3} - \frac{4}{3}y + y^2 \right) \times [Z^2 (\varphi_1 - \frac{4}{3} \ln Z - 4f) + Z(\psi_1 - \frac{8}{3} \ln Z)] + \frac{2}{3}(1-y)[Z^2(\varphi_1 - \varphi_2) + Z(\psi_1 - \psi_2)] \right\}$$

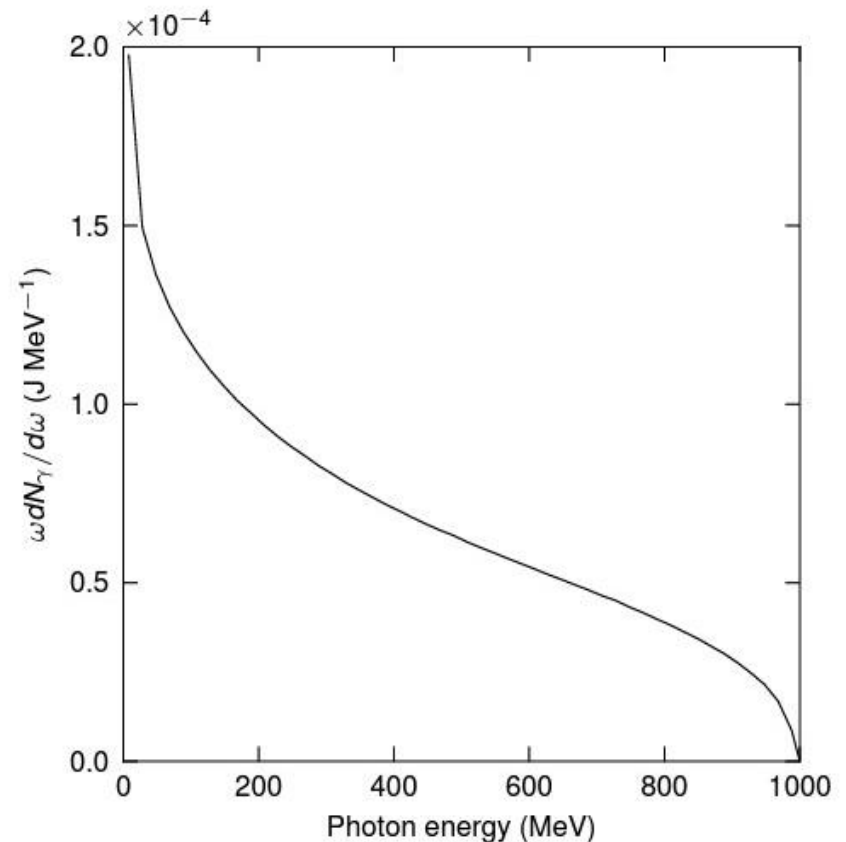
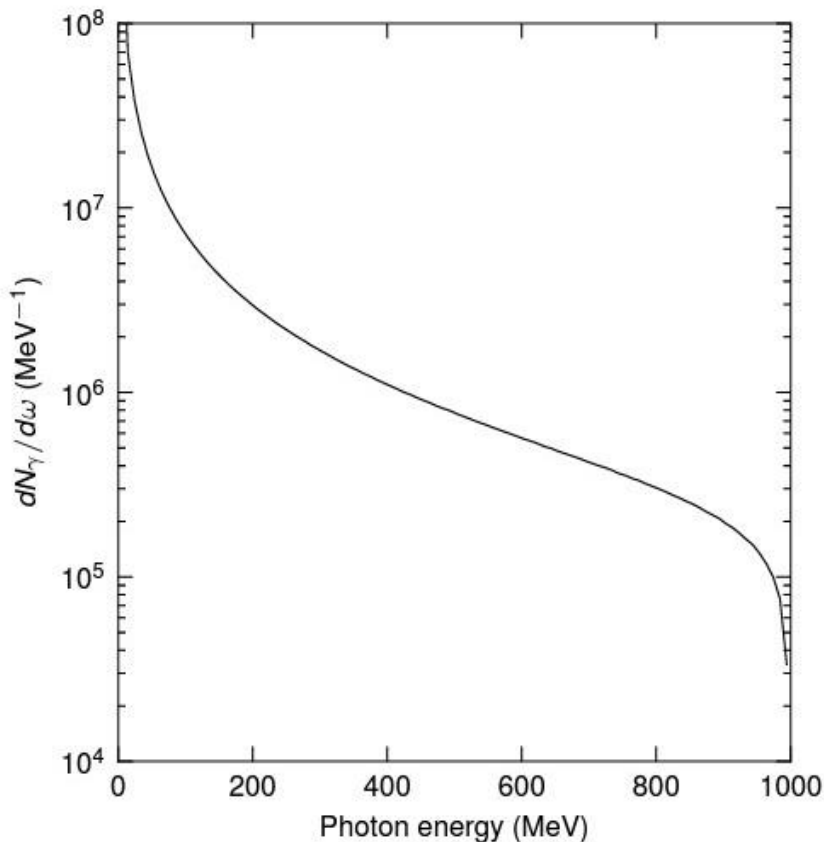
- Emitted photons pair produce, resulting in cascades of low energy particles
- For maximum conversion to ultra high-energy photons, optimal target width a few mm

Pike et al., *Nature Photonics* **8**, 434 (2014)

2. Bremsstrahlung γ -ray energy distribution

The distribution of gamma-rays leaving target is broad, but a significant number of them have very high energies

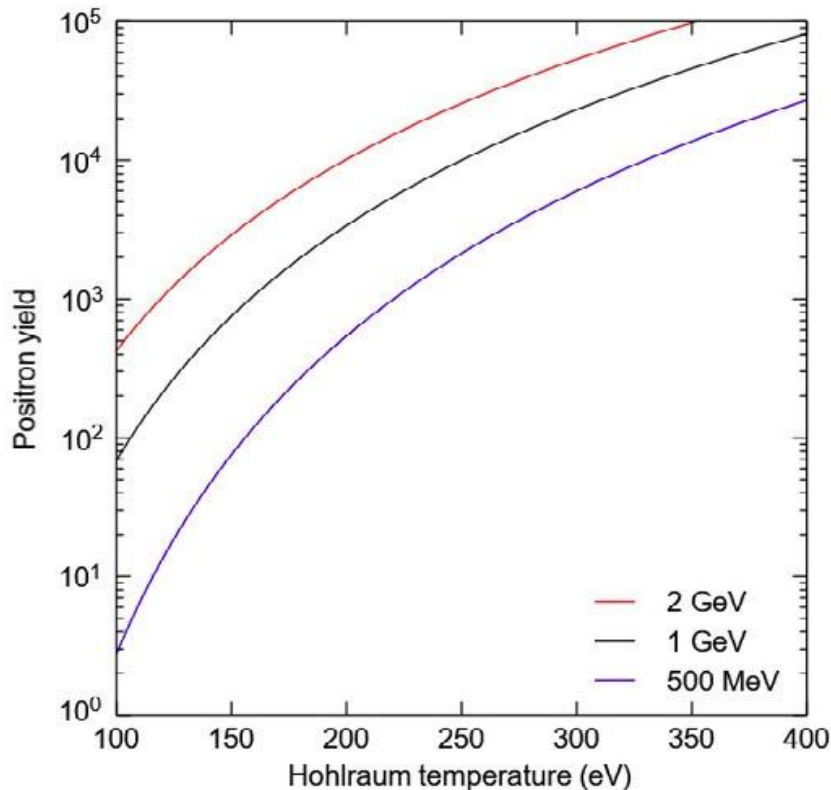
Distribution of photons leaving back surface of gold converter (3 mm thick)



2. Breit-Wheeler pair production

Significant Breit-Wheeler pair production expected over wide range of beam energies and hohlraum temperatures

Number of positrons formed in hohlraum (length 1 cm)



- Number of Breit-Wheeler positrons formed in hohlraum given by

$$N_{e^+} \sim N_{\gamma_1} n_{\gamma_2} \delta x \cdot \sigma$$

where

$$N_{\gamma_1} \sim 10^9 \quad \text{Gamma-ray number}$$

$$n_{\gamma_2} \sim 10^{27} \text{ m}^{-3} \quad \text{X-ray number density}$$

$$\delta x \sim 10^{-2} \text{ m} \quad \text{Length of hohlraum}$$

$$\sigma \sim 10^{-29} \text{ m}^2 \quad \text{Breit-Wheeler cross-section}$$

for a hohlraum of temperature 400 eV, leading to up to

$$N_{e^+} \sim 10^5$$

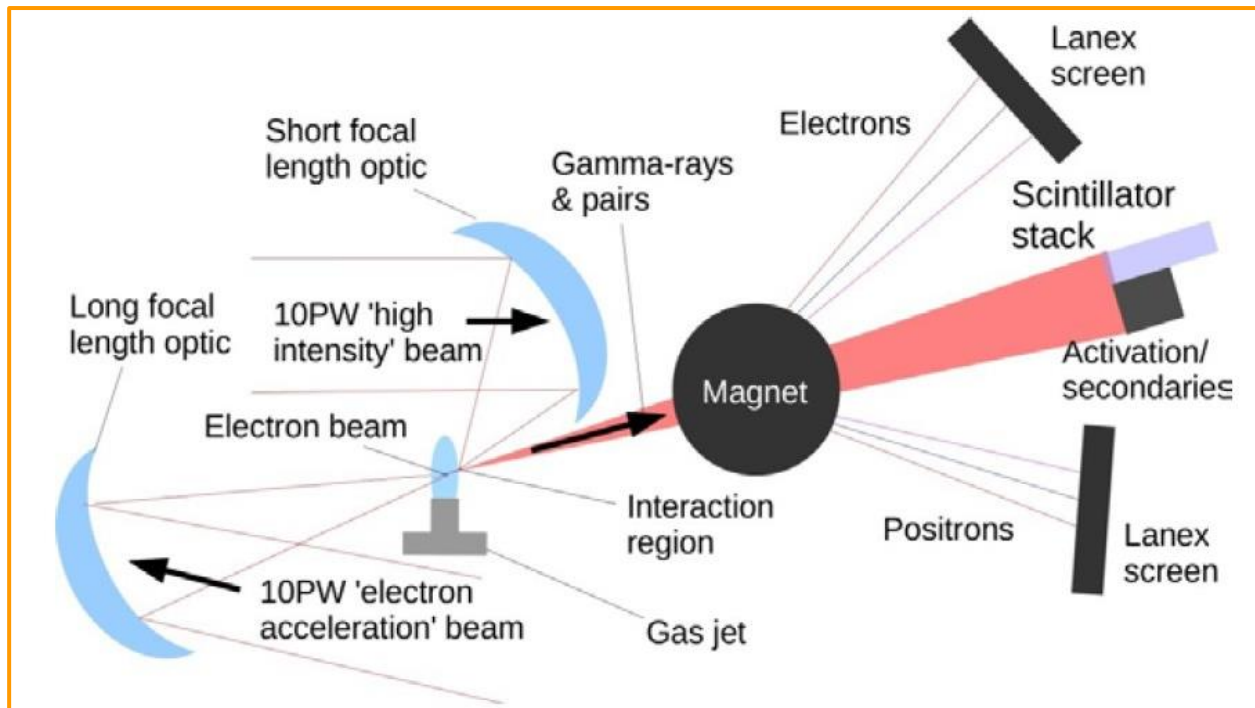
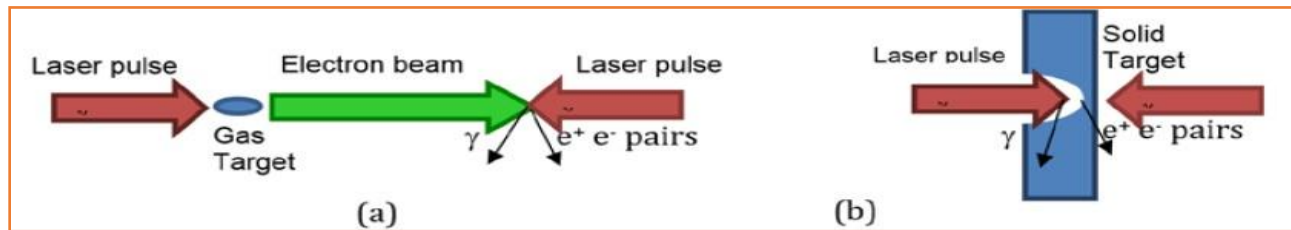
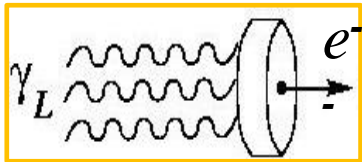
events per shot

2. ELI-NP possibility to study QED Processes

I.C.E. Turcu et al, "High field physics and QED experiments at ELI-NP", Rom. Rep. Phys. 68, Supplement, S145 (2016).

- ELI-NP facility will enable for the first time the use of two 10 PW laser beams for QED experiments.
- The first beam will accelerate electrons to relativistic energies.
 - The second beam will subject relativistic electrons to the strong electromagnetic field generating QED processes: intense gamma ray radiation and electron-positron pair formation.

Wakefield acceleration



2. ELI-NP possibility to study QED Processes

I.C.E. Turcu et al, “High field physics and QED experiments at ELI-NP”, Rom. Rep. Phys. 68, Supplement, S145 (2016).

We propose to use the unique capabilities of ELI-NP to:

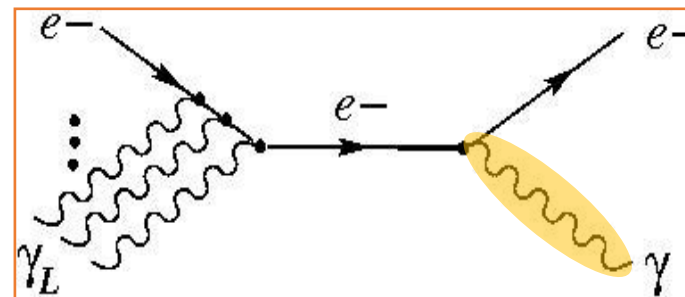
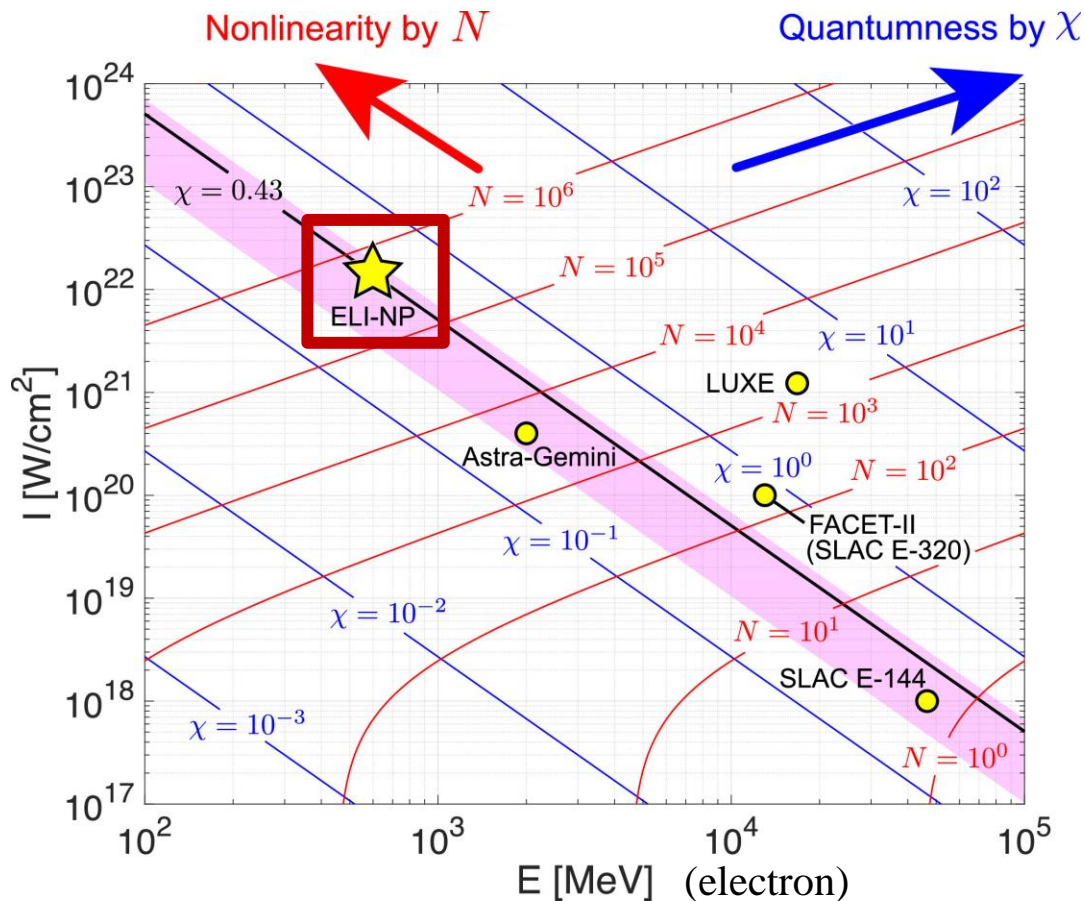
1. Observe the transition to the very **nonlinear Compton scattering** regime,
2. Measure the cross-section for strongly **nonlinear Breit-Wheeler pair production**.
3. Measure the cross-section for the **(nonlinear) Bethe-Heitler pair production**.

The experimental area E6 at ELI-NP is ready for investigating high field physics and QED for production of electron-positron-pairs and of energetic gamma-rays.

Two pump-probe colliding 10 PW laser beams are proposed for the E6 interaction chamber. The focused pump laser beam accelerates the electrons to relativistic energies. The accelerated electron bunches interact with the very high EM field of the focused probe laser beam.

Proposed two main types of experiments with: (a) ***gas targets*** in which the pump laser-beam is focused by a long focal length mirror and drives a wakefield in which the electron bunch is accelerated to multi-GeV energies and then exposed to the EM field of the probe laser which is tightly focused; (b) ***solid targets*** in which both the pump and probe laser beams are focused on the solid target, one accelerating the electrons in the solid and the other, delayed, providing the high electric field to which the relativistic electrons are subjected.

2. ELI-NP possibilities (K.Seto 2021)



Before collision (e + laser)

$$\begin{pmatrix} E \\ p \end{pmatrix} + N \times \begin{pmatrix} \hbar\omega \\ \hbar k \end{pmatrix} = \begin{pmatrix} E' \\ p' \end{pmatrix} + \begin{pmatrix} \hbar\omega' \\ \hbar k' \end{pmatrix}$$

After collision (e + gamma)

$$\chi \propto \hbar \times \text{electron energy } (E) \times \sqrt{\text{laser intensity } (I)}.$$

$$N \propto \frac{\hbar\omega'}{E - \hbar\omega'} \times \frac{I}{E}, \quad \hbar\omega' = \frac{E}{2}.$$

So, consider the uses of photons from 10 keV to GeV-class !

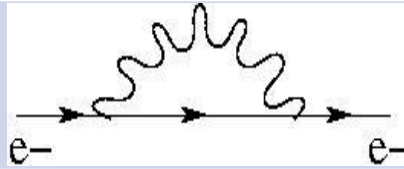
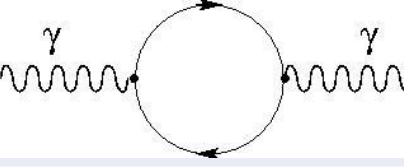

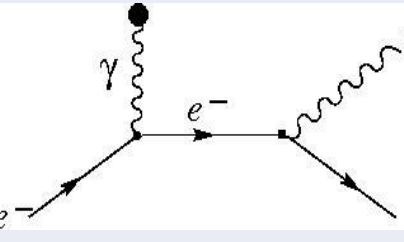
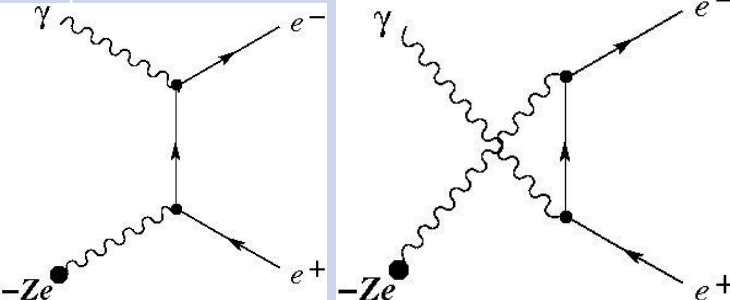
(K. Seto, Seminar 2021)

The physical regime diagram of RR. The curves at given N and χ are shown in the diagram. N is the number of absorbed laser photon and χ is intensity parameter. Here, an emitted photon energy $\hbar\omega'$ is selected as $\hbar\omega' = E/2$ for an electron energy E , $\theta_{in} = 155^\circ$ and $\hbar\omega = 1.5$ eV are taken into account to estimate where the proposed **experiment at ELI-NP** is. The pink ribbon represents the domain as $\chi \in [0.2, 0.5]$. We consider “linear” Compton scattering in the area where $N \leq 1$ (a single laser photon absorption) by given $\hbar\omega'$ and E . The star symbol shows the parameter set at ELI-NP. (K. Seto, Seminar 2021)

3. QED processes

QED PROCESS	INTERACTION	S MATRIX ELEMENT
Compton Scattering $e^- \gamma$		$\langle \gamma, e^- S \gamma, e^- \rangle \quad \langle \gamma, e^+ S \gamma, e^+ \rangle$
Dirac pair annihilation $e^+ e^-$		$\langle \gamma, \gamma S e^-, e^+ \rangle$
Breit-Wheeler pair production $e^+ e^-$		$\langle e^-, e^+ S \gamma, \gamma \rangle$
Moller Scattering $e^- e^-$		$\langle e^-, e^- S e^-, e^- \rangle \quad \langle e^+, e^+ S e^+, e^+ \rangle$
Bhabha Scattering		$\langle e^-, e^+ S e^-, e^+ \rangle$

3. QED processes

QED PROCESS	INTERACTION	S MATRIX ELEMENT
Electron Self Energy		$\langle e^- S e^- \rangle \quad \langle e^+ S e^+ \rangle$
Photon Self Energy		$\langle \gamma S \gamma \rangle$
Vacuum Energy		$\langle 0 S 0 \rangle$
Bremsstrahlung		$\langle \gamma, e^- S \gamma_V, e^- \rangle$
Bethe-Heitler		$\langle e^-, e^+ S \gamma, \gamma_V \rangle$

3. Feynman Diagrams QED Processes

PROCES	INTERACTIA	ELEMENT MATRICE \hat{S}
Imprăștiere foton-electron $\gamma + e^- \rightarrow \gamma + e^-$		$\langle \gamma, e^- \hat{S} \gamma, e^- \rangle$
Imprăștiere foton-pozitron $\gamma + e^+ \rightarrow \gamma + e^+$		$\langle \gamma, e^+ \hat{S} \gamma, e^+ \rangle$
Anihilare perechi e^+e^- $e^- + e^+ \rightarrow \gamma + \gamma$		$\langle \gamma, \gamma \hat{S} e^-, e^+ \rangle$
Producere perechi e^+e^- $\gamma + \gamma \rightarrow e^- + e^+$		$\langle e^-, e^+ \hat{S} \gamma, \gamma \rangle$
Imprăștierea Möller e^- $e^- + e^- \rightarrow e^- + e^-$		$\langle e^-, e^- \hat{S} e^-, e^- \rangle$
Imprăștierea Möller e^+ $e^+ + e^+ \rightarrow e^+ + e^+$		$\langle e^+, e^+ \hat{S} e^+, e^+ \rangle$

PROCES	INTERACTIA	ELEMENT MATRICE \hat{S}
Imprăștierea Bhabha $e^- + e^+ \rightarrow e^- + e^+$		$\langle e^-, e^+ \hat{S} e^-, e^+ \rangle$
Energie proprie electron $e^- \rightarrow e^-$		$\langle e^- \hat{S} e^- \rangle$
Energie proprie pozitron $e^+ \rightarrow e^+$		$\langle e^+ \hat{S} e^+ \rangle$
Energie proprie foton $\gamma \rightarrow \gamma$		$\langle \gamma \hat{S} \gamma \rangle$
Energie vacuum Vacuum \rightarrow Vacuum		$\langle 0 \hat{S} 0 \rangle$

$$\left\{ \begin{aligned}
 \hat{A}_\mu(x) &= \int \frac{d^3\vec{k}}{(2\pi)^3} \frac{1}{2\omega} \left[\underbrace{\hat{a}_\lambda(\vec{k}) \epsilon_\mu^\lambda e^{-ik \cdot x}}_{\sim \hat{A}_\mu^-(x)} + \underbrace{\hat{a}_\lambda^\dagger(\vec{k}) \epsilon_\mu^\lambda e^{ik \cdot x}}_{\sim \hat{A}_\mu^+(x)} \right] \\
 \hat{\psi}(x) &= \int \frac{d^3\vec{p}}{(2\pi)^3} \frac{m}{\omega} \left[\underbrace{\hat{b}(\vec{p}) u(\vec{p}) e^{-ip \cdot x}}_{\sim \hat{\psi}^-(x)} + \underbrace{\hat{c}^\dagger(\vec{p}) v(\vec{p}) e^{ip \cdot x}}_{\sim \hat{\psi}^+(x)} \right] \\
 \hat{\bar{\psi}}(x) &= \int \frac{d^3\vec{p}}{(2\pi)^3} \frac{m}{\omega} \left[\underbrace{\hat{c}(\vec{p}) \bar{v}(\vec{p}) e^{-ip \cdot x}}_{\sim \hat{\bar{\psi}}^-(x)} + \underbrace{\hat{b}^\dagger(\vec{p}) \bar{u}(\vec{p}) e^{ip \cdot x}}_{\sim \hat{\bar{\psi}}^+(x)} \right]
 \end{aligned} \right.$$

$\hat{A}_\mu^-(x) \rightarrow \hat{a}$ - anihilare foton în x

$\hat{A}_\mu^+(x) \rightarrow \hat{a}^\dagger$ - creare foton în x

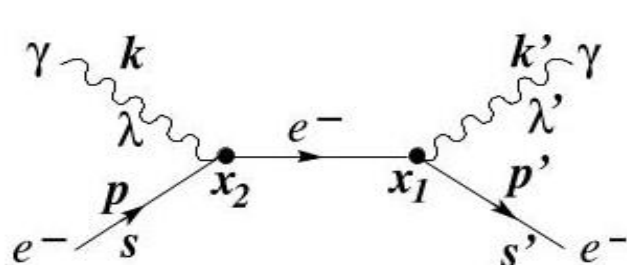
$\hat{\psi}^-(x) \rightarrow \hat{b}$ - anihilare electron în x

$\hat{\psi}^+(x) \rightarrow \hat{c}^\dagger$ - creare pozitron în x

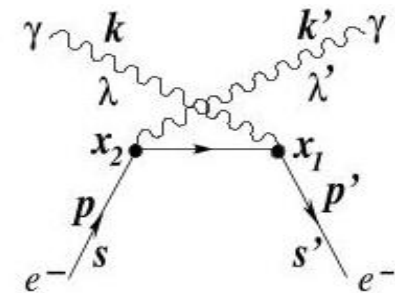
$\hat{\bar{\psi}}^-(x) \rightarrow \hat{c}$ - anihilare pozitron în x

$\hat{\bar{\psi}}^+(x) \rightarrow \hat{b}^\dagger$ - creare electron în x

3. Feynman Diagrams: $\gamma - e^-$ scattering



$$\langle \gamma, e^- | \hat{S}_A | \gamma, e^- \rangle$$



$$\langle \gamma, e^- | \hat{S}_B | \gamma, e^- \rangle$$

- Folosind componentele corespunzătoare de creare/anihilare din $\hat{\psi}(x)$, $\hat{\bar{\psi}}(x)$ și $\hat{A}_\mu(x)$

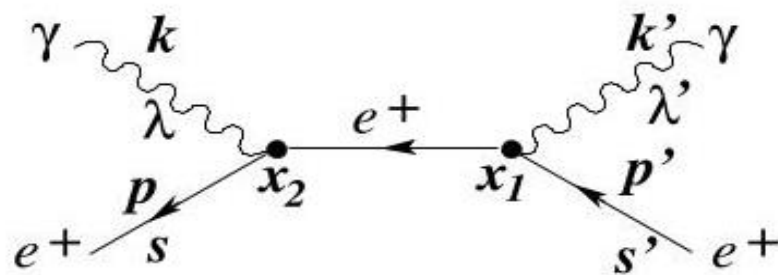
$$\hat{S}_A = - \left(\frac{e}{\hbar} \right)^2 \int d^4x_1 d^4x_2 N \left[\begin{array}{cccccc} \text{crea.} & \text{crea.} & & & \text{anih.} & \text{anih.} \\ e^- & \gamma' & & & \gamma & e^- \\ \downarrow & \downarrow & & & \downarrow & \downarrow \\ (\hat{\psi}_{x_1}^+) & (\hat{A}_{x_1}^+) & \underbrace{(\hat{\psi}_{x_1}^-) (\hat{\psi}_{x_2}^+)}_{iS_F(x_1-x_2)} & & (\hat{A}_{x_2}^-) & (\hat{\psi}_{x_2}^-) \end{array} \right]$$

$$\hat{S}_B = - \left(\frac{e}{\hbar} \right)^2 \int d^4x_1 d^4x_2 N \left[\begin{array}{cccccc} \text{crea.} & \text{anih.} & & & \text{crea.} & \text{anih.} \\ e^- & \gamma & & & \gamma' & e^- \\ \downarrow & \downarrow & & & \downarrow & \downarrow \\ (\hat{\psi}_{x_1}^+) & (\hat{A}_{x_1}^-) & \underbrace{(\hat{\psi}_{x_1}^-) (\hat{\psi}_{x_2}^+)}_{iS_F(x_1-x_2)} & & (\hat{A}_{x_2}^+) & (\hat{\psi}_{x_2}^-) \end{array} \right]$$

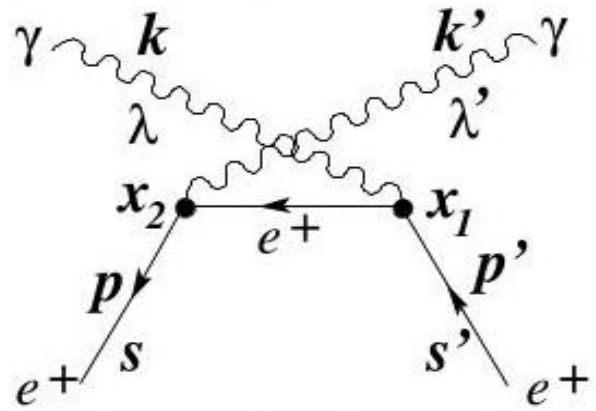
$$\langle \gamma, e^- | \hat{S}_{ge}^{(2)} | \gamma, e^- \rangle = (2\pi)^4 \delta^4(p+k-p'-k') \mathcal{M}_{fi}$$

$$\left\{ \begin{array}{l} \mathcal{M}_{fi} = \mathcal{M}_{fi}^A + \mathcal{M}_{fi}^B \\ \mathcal{M}_{fi}^A = - \left(\frac{e}{\hbar} \right)^2 \bar{u}_{s'}(\vec{p}') \not{\epsilon}_{\lambda'} iS_F(p+k) \not{\epsilon}_\lambda u_s(\vec{p}) \\ \mathcal{M}_{fi}^B = - \left(\frac{e}{\hbar} \right)^2 \bar{u}_{s'}(\vec{p}') \not{\epsilon}_{\lambda'} iS_F(p-k') \not{\epsilon}_\lambda u_s(\vec{p}) \end{array} \right.$$

3. Feynman Diagrams: $\gamma - e^+$ scattering



$$\langle \gamma, e^+ | \hat{S}_A | \gamma, e^+ \rangle$$



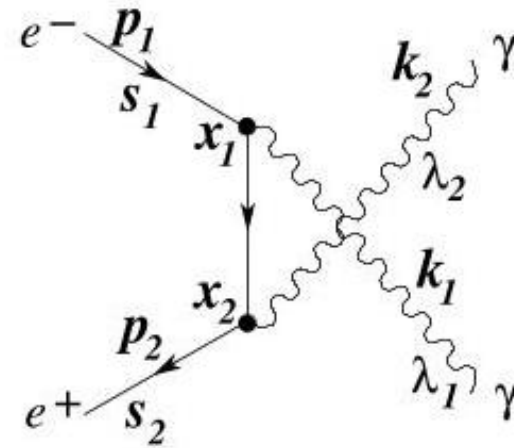
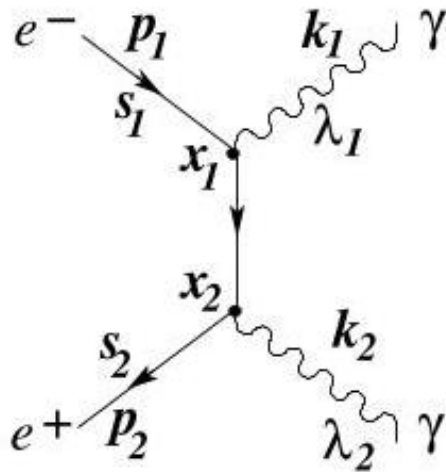
$$\langle \gamma, e^+ | \hat{S}_B | \gamma, e^+ \rangle$$

- Folosind componentele corespunzătoare de creare/anihilare din $\hat{\psi}(x)$, $\hat{\bar{\psi}}(x)$ și $\hat{A}_\mu(x)$

$$\hat{S}_A = - \left(\frac{e}{\hbar} \right)^2 \int d^4x_1 d^4x_2 N \left[\begin{array}{cccc} \text{crea. } e^+ & \text{crea. } \gamma' & & \text{anih. } \gamma & \text{anih. } e^+ \\ \downarrow & \downarrow & & \downarrow & \downarrow \\ (\hat{\psi}_{x_1}^+) & (\hat{A}_{x_1}^+) & \underbrace{(\hat{\psi}_{x_1}^-) (\hat{\psi}_{x_2}^+)}_{iS_F(x_1-x_2)} & (\hat{A}_{x_2}^-) & (\hat{\psi}_{x_2}^-) \end{array} \right]$$

$$\hat{S}_B = - \left(\frac{e}{\hbar} \right)^2 \int d^4x_1 d^4x_2 N \left[\begin{array}{cccc} \text{crea. } e^+ & \text{anih. } \gamma & & \text{crea. } \gamma' & \text{anih. } e^+ \\ \downarrow & \downarrow & & \downarrow & \downarrow \\ (\hat{\psi}_{x_1}^+) & (\hat{A}_{x_1}^-) & \underbrace{(\hat{\psi}_{x_1}^-) (\hat{\psi}_{x_2}^+)}_{iS_F(x_1-x_2)} & (\hat{A}_{x_2}^+) & (\hat{\psi}_{x_2}^-) \end{array} \right]$$

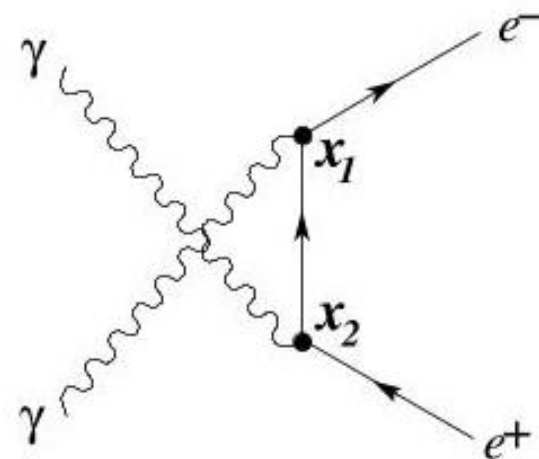
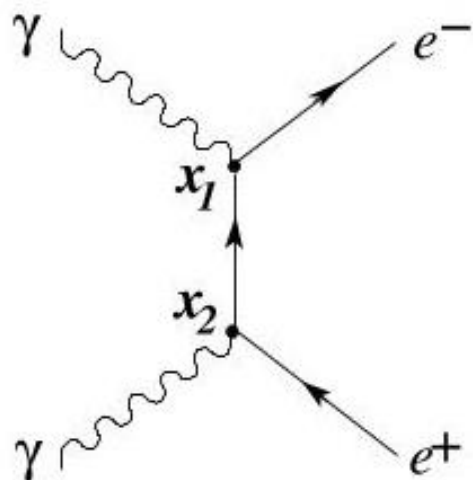
3. Feynman Diagrams Pair Annihilation: $e^-e^+ \rightarrow \gamma\gamma$



- Folosind componentele corespunzătoare de creare/anihilare din $\hat{\psi}(x)$, $\hat{\bar{\psi}}(x)$ și $\hat{A}_\mu(x)$

$$\hat{S}_{ap}^{(2)} = - \left(\frac{e}{\hbar} \right)^2 \int d^4x_1 d^4x_2 N \left[\begin{array}{cccccc} \text{anih.} & \text{crea.} & & & \text{crea.} & \text{anih.} \\ e^- & \gamma & & & \gamma & e^+ \\ \downarrow & \downarrow & & & \downarrow & \downarrow \\ \left(\hat{\psi}_{x_1}^- \right) & \left(\hat{A}_{x_1}^+ \right) & \underbrace{\left(\hat{\psi}_{x_1}^- \right) \left(\hat{\bar{\psi}}_{x_2}^+ \right)}_{iS_F(x_1-x_2)} & & \left(\hat{A}_{x_2}^+ \right) & \left(\hat{\bar{\psi}}_{x_2}^- \right) \end{array} \right]$$

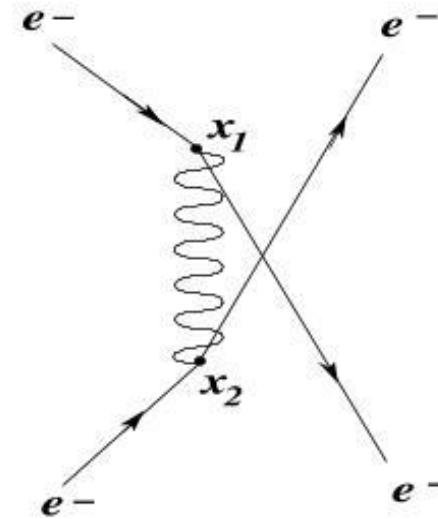
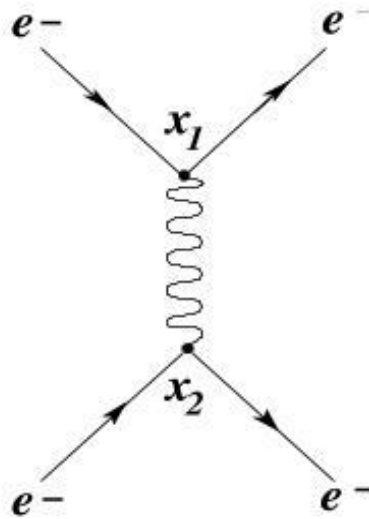
3. Feynman Diagrams Pair Production (Breit-Wheeler): $\gamma \gamma \rightarrow e^- e^+$



- Folosind componentele corespunzătoare de creare/anihilare din $\hat{\psi}(x)$, $\hat{\bar{\psi}}(x)$ și $\hat{A}_\mu(x)$

$$\hat{S}_{pp}^{(2)} = - \left(\frac{e}{\hbar} \right)^2 \int d^4x_1 d^4x_2 N \left[\begin{array}{cccccc} \text{crea. } e^- & \text{anih. } \gamma & & & \text{anih. } \gamma & \text{crea. } e^+ \\ \downarrow & \downarrow & & & \downarrow & \downarrow \\ \left(\hat{\bar{\psi}}_{x_1}^+ \right) & \left(\hat{A}_{x_1}^- \right) & \overbrace{\left(\hat{\psi}_{x_1}^- \right) \left(\hat{\bar{\psi}}_{x_2}^+ \right)} & & \left(\hat{A}_{x_2}^- \right) & \left(\hat{\psi}_{x_2}^+ \right) \\ & & iS_F(x_1-x_2) & & & \end{array} \right]$$

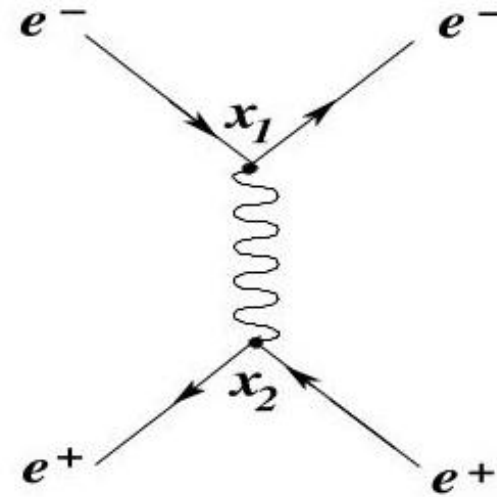
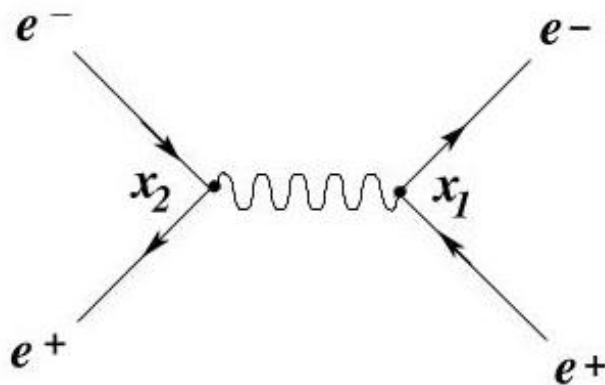
3. Feynman Diagrams Moller Scattering: $e^- e^- \rightarrow e^- e^-$



- Folosind componentele corespunzătoare de creare/anihilare din $\hat{\psi}(x)$, $\hat{\bar{\psi}}(x)$ și $\hat{A}_\mu(x)$

$$\hat{S}_{mse}^{(2)} = - \left(\frac{e}{\hbar} \right)^2 \int d^4x_1 d^4x_2 N \left[\begin{array}{cccccc} \text{crea.} & \text{anih.} & & & \text{crea.} & \text{anih.} \\ e^- & e^- & & & e^- & e^- \\ \downarrow & \downarrow & & & \downarrow & \downarrow \\ \left(\hat{\bar{\psi}}_{x_1}^+ \right) & \left(\hat{\psi}_{x_1}^- \right) & \underbrace{\left(\hat{A}_{x_1}^- \right) \left(\hat{A}_{x_2}^+ \right)}_{D_F(x_1-x_2)} & & \left(\hat{\bar{\psi}}_{x_2}^+ \right) & \left(\hat{\psi}_{x_2}^- \right) \end{array} \right]$$

2. Feynman Diagrams Bhabha Scattering: $e^- e^+ \rightarrow e^- e^+$

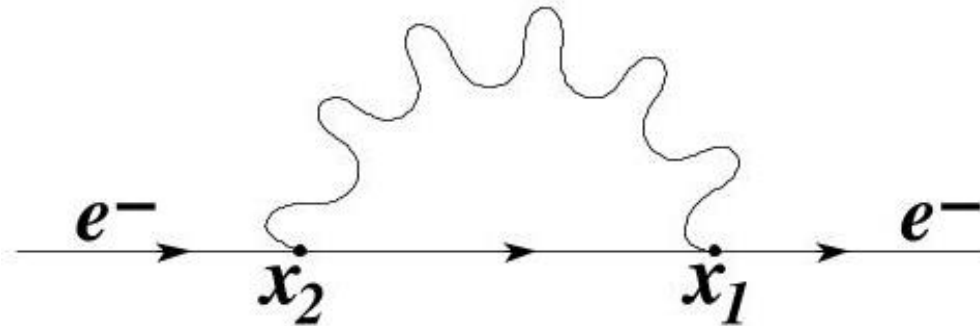


- Folosind componentele corespunzătoare de creare/anihilare din $\hat{\psi}(x)$, $\hat{\bar{\psi}}(x)$ și $\hat{A}_\mu(x)$

$$\hat{S}_A = - \left(\frac{e}{\hbar} \right)^2 \int d^4x_1 d^4x_2 N \left[\begin{array}{cccccc} \text{crea.} & \text{crea.} & & & \text{anih.} & \text{anih.} \\ e^- & e^+ & & & e^+ & e^- \\ \downarrow & \downarrow & & & \downarrow & \downarrow \\ \left(\hat{\bar{\psi}}_{x_1}^+ \right) & \left(\hat{\psi}_{x_1}^+ \right) & \underbrace{\left(\hat{A}_{x_1}^- \right) \left(\hat{A}_{x_2}^+ \right)}_{D_F(x_1-x_2)} & & \left(\hat{\bar{\psi}}_{x_2}^- \right) & \left(\hat{\psi}_{x_2}^- \right) \end{array} \right]$$

$$\hat{S}_B = - \left(\frac{e}{\hbar} \right)^2 \int d^4x_1 d^4x_2 N \left[\begin{array}{cccccc} & \text{anih.} & \text{crea.} & & \text{crea.} & \text{anih.} \\ & e^- & e^- & & e^+ & e^+ \\ & \downarrow & \downarrow & & \downarrow & \downarrow \\ & \left(\hat{\bar{\psi}}_{x_1}^- \right) & \left(\hat{\psi}_{x_1}^+ \right) & \underbrace{\left(\hat{A}_{x_1}^- \right) \left(\hat{A}_{x_2}^+ \right)}_{D_F(x_1-x_2)} & \left(\hat{\psi}_{x_2}^+ \right) & \left(\hat{\bar{\psi}}_{x_2}^- \right) \end{array} \right]$$

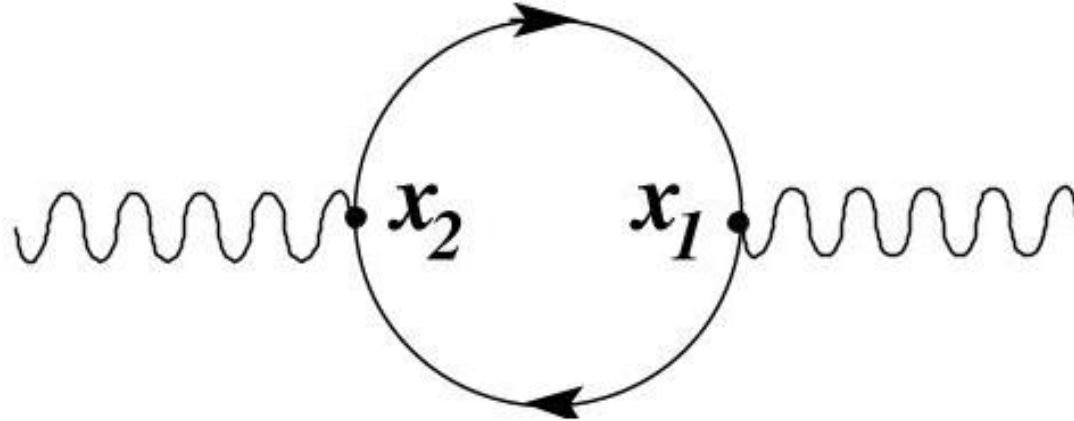
3. Feynman Diagrams: Electron Self Energy



- Folosind componentele corespunzătoare de creare/anihilare din $\hat{\psi}(x)$, $\hat{\bar{\psi}}(x)$ și $\hat{A}_\mu(x)$

$$\hat{S}_{see}^{(2)} = \frac{(-ie/\hbar)^2}{2!} \int d^4x_1 d^4x_2 N \left[\begin{array}{c} \text{crea.} \\ e^- \\ \downarrow \\ (\hat{\bar{\psi}}_{x_1}^+) \end{array} \underbrace{(\hat{\psi}_{x_1}^-)(\hat{\bar{\psi}}_{x_2}^+)}_{iS_F(x_1-x_2)} \underbrace{(\hat{A}_{x_1}^-)(\hat{A}_{x_2}^+)}_{D_F(x_1-x_2)} \begin{array}{c} \text{anih.} \\ e^- \\ \downarrow \\ (\hat{\bar{\psi}}_{x_2}^-) \end{array} \right]$$

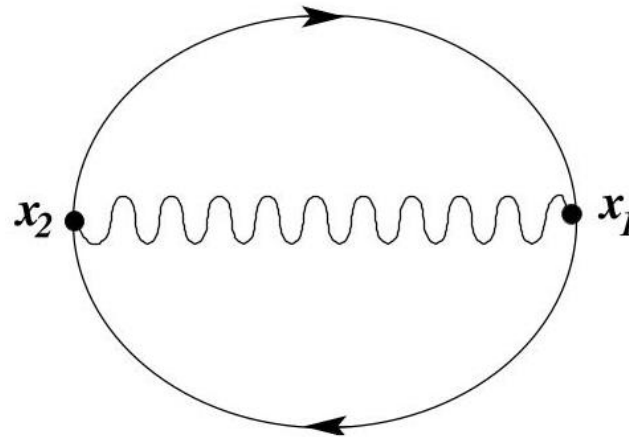
3. Feynman Diagrams: Photon Self Energy



- Folosind componentele corespunzătoare de creare/anihilare din $\hat{\psi}(x)$, $\hat{\bar{\psi}}(x)$ și $\hat{A}_\mu(x)$

$$\hat{S}_{seg}^{(2)} = - \left(\frac{e}{\hbar} \right)^2 \int d^4x_1 d^4x_2 N \left(Tr \left[\underbrace{\left(\hat{\psi}_{x_1}^- \right) \left(\hat{\bar{\psi}}_{x_2}^+ \right)}_{iS_F(x_1-x_2)} \overset{\text{crea.}}{\underset{\gamma}{\downarrow}} \hat{A}_{x_1}^+ \underbrace{\left(\hat{\psi}_{x_1}^- \right) \left(\hat{\bar{\psi}}_{x_2}^+ \right)}_{iS_F(x_1-x_2)} \overset{\text{anih.}}{\underset{\gamma}{\downarrow}} \hat{A}_{x_2}^- \right] \right)$$

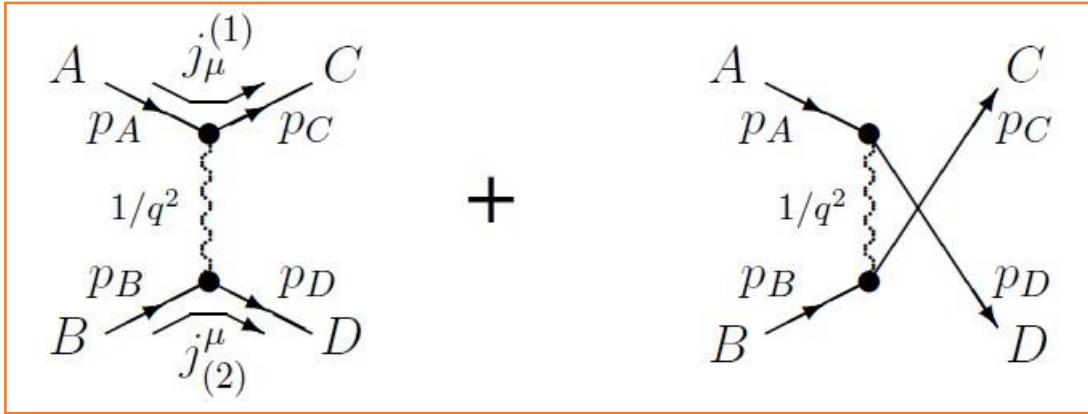
3. Feynman Diagrams: Vacuum Energy



- Folosind componentele corespunzătoare de creare/anihilare din $\hat{\psi}(x)$, $\hat{\bar{\psi}}(x)$ și $\hat{A}_\mu(x)$

$$\hat{S}_{sev}^{(2)} = \frac{(-ie/\hbar)^2}{2!} \int d^4x_1 d^4x_2 N \left(Tr \left[\underbrace{\hat{\psi}_{x_2}^- \hat{\psi}_{x_1}^+}_{iS_F(x_2-x_1)} \underbrace{\hat{\psi}_{x_1}^- \hat{\psi}_{x_2}^+}_{iS_F(x_1-x_2)} \underbrace{\hat{A}_{x_1}^- \hat{A}_{x_2}^+}_{D_F(x_1-x_2)} \right] \right)$$

3. Feynman diagrams evaluation (example - Moller e^-e^- Scattering)



$$\left. \frac{d\sigma}{d\Omega} \right|_{scm} = \frac{1}{64\pi^2 s} \frac{|\vec{p}_f|}{|\vec{p}_i|} |\mathcal{M}|^2$$

$$-i\mathcal{M} = \left(i e \bar{u}_C \gamma^\mu u_A \right) \left(\frac{-i g_{\mu\nu}}{q^2} \right) \left(i e \bar{u}_D \gamma^\mu u_B \right)$$

$$\mathcal{M} = - e^2 \frac{(\bar{u}_C \gamma_\mu u_A)(\bar{u}_D \gamma^\mu u_B)}{(p_C - p_A)^2} + e^2 \frac{(\bar{u}_D \gamma_\mu u_A)(\bar{u}_C \gamma^\mu u_B)}{(p_D - p_A)^2}$$

$$|\mathcal{M}|^2 \longrightarrow \overline{|\mathcal{M}|^2} \equiv \frac{1}{(2s_A + 1)(2s_B + 1)} \sum_{\text{toate stările de spin}} |\mathcal{M}|^2$$

$$\left. \frac{d\sigma}{d\Omega} \right|_{scm} = \frac{1}{64\pi^2 s} \frac{|\vec{p}_f|}{|\vec{p}_i|} \overline{|\mathcal{M}|^2} = \frac{m^2 c^4 \alpha^2}{16p^4} \left(\frac{1}{\sin^4 \frac{\theta}{2}} + \frac{1}{\cos^4 \frac{\theta}{2}} - \frac{1}{\sin^2 \frac{\theta}{2} \cos^2 \frac{\theta}{2}} \right)$$

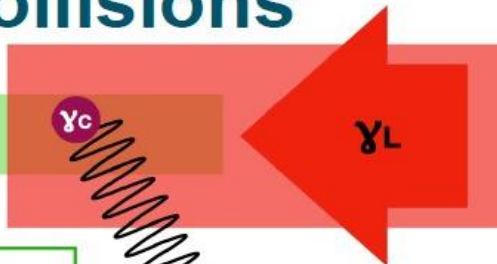
4. Upcoming Experiments

- The LoI to Theory Frontier (2020) [12] proposes to explore strong-field QED predictions for new experiments in the $\chi > 1$ regime, which could provide High-Energy-Density Physics (HEDP) by a 30 GeV electron beam at interacting with a multi-Petawatt laser and a high-intensity short bunch beam-beam collisions [21–24].
- There are several initiatives to explore **nonperturbative effects** with respect to the laser field [15]. These include upcoming experiments at
 - **DESY (LUXE)** [16],
 - **SLAC (E-320 at FACET II)** [17]
 - **National Ignition Facility** (USA) [28], with the Titan laser, one of the two lasers in the Jupiter facility.
- possible at our **ELI-NP** laser facility [18]. The opportunity to create such beam-laser photon collisions has been strongly endorsed by both the high intensity laser [19] and the plasma physics community [20]. These experiments will enable precision comparisons of theory and experiment in strong-field regimes.

4. LUXE at DESY: electron - laser interaction studies

LUXE: electron-laser collisions

High-energy electrons
(16.5 GeV XFEL beam)



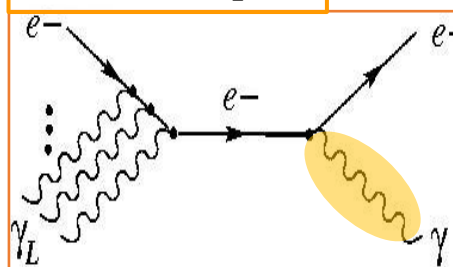
High-intensity LASER
(Tera-Watt, 800nm)
→ large E-field

note: in reality, LASER
crossing angle $\theta=17.2^\circ$

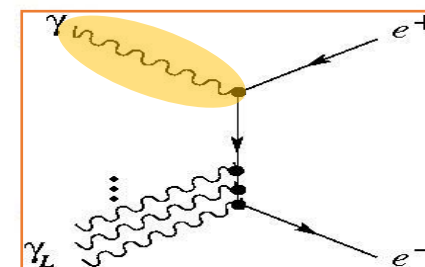
Lorentz boost:
electrons “see” larger
E-field of the LASER
in their rest frame:
 $E^* = \gamma_e \mathcal{E}_L (1 + \cos \theta)$

**electron-positron
pair production**

Inverse Compton



+



Physics processes:

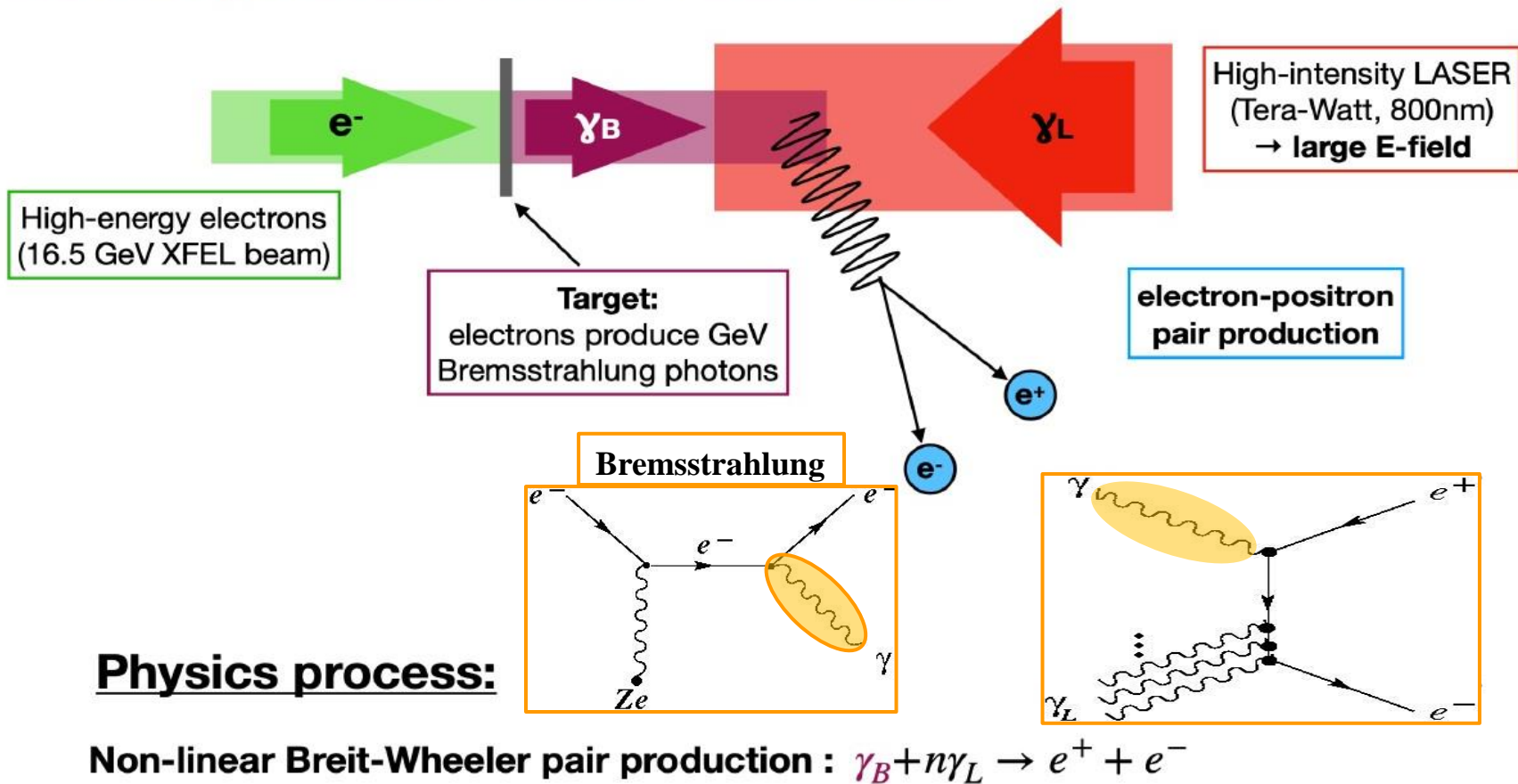
- 1 Non-linear Compton Scattering: $e^- + n\gamma_L \rightarrow e^- + \gamma_C$
- 2 Non-linear Breit-Wheeler pair production: $\gamma_C + n\gamma_L \rightarrow e^+ + e^-$

• LUXE main goals:

- ➔ Measure Compton scattering (and edge position) versus laser intensity.
- ➔ Measure positron rate versus laser intensity.

4. LUXE at DESY: electron - laser interaction studies

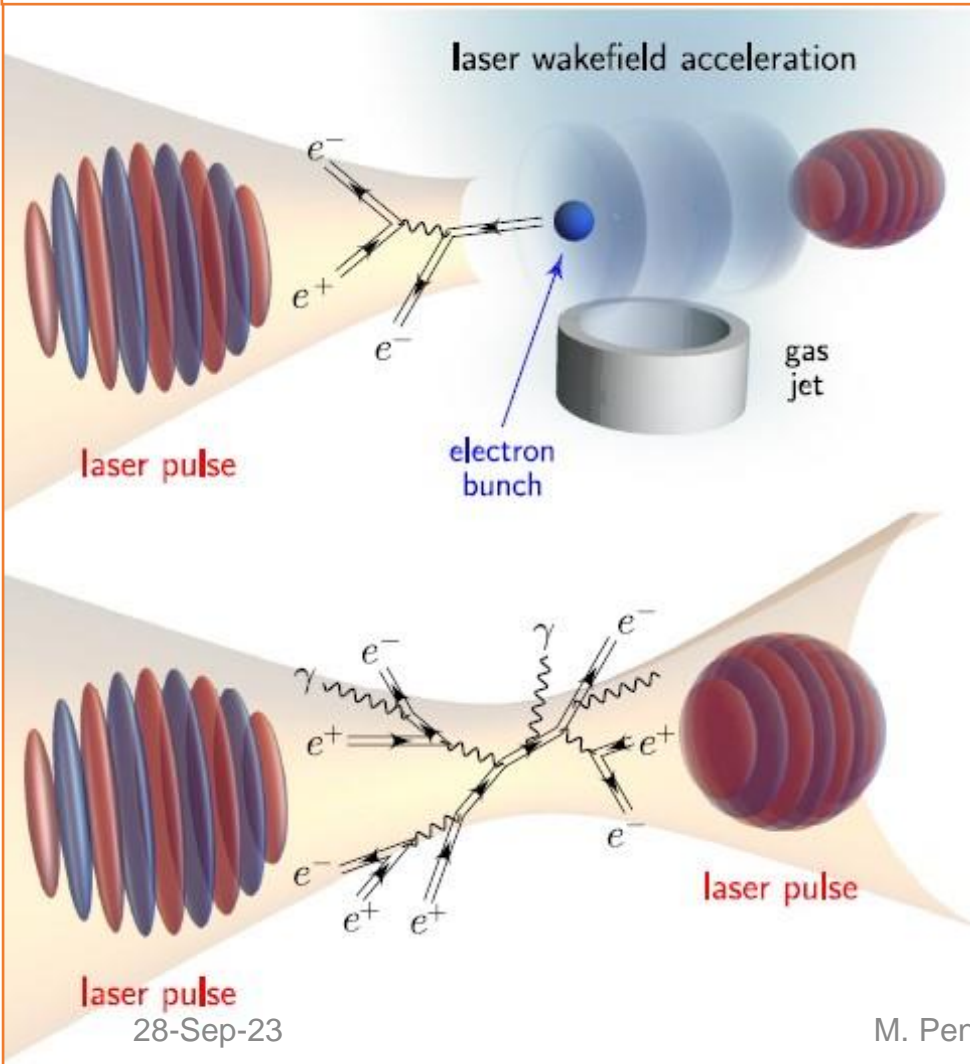
LUXE: photon-laser collisions



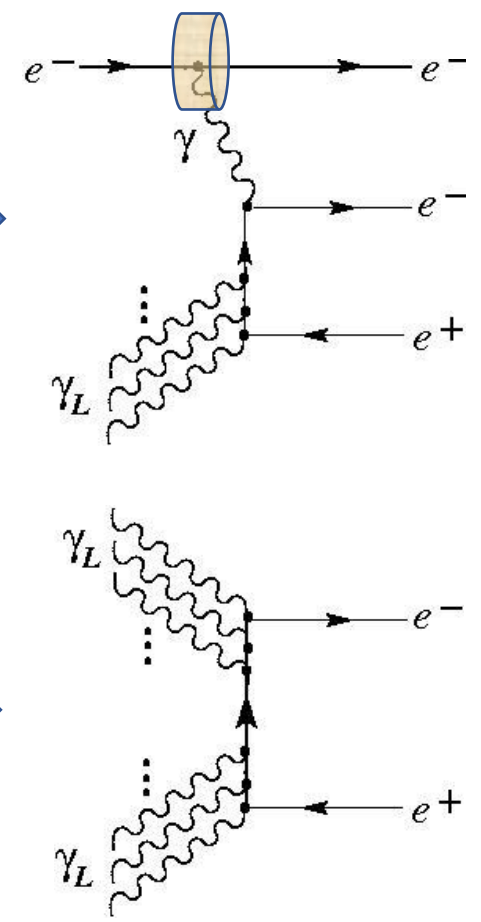
4. Competitive projects: Simulation laser - laser interaction

Charged particle motion and radiation in strong electromagnetic fields

A. Gonoskov, T. G. Blackburn, M. Marklund, S. S. Bulanov
 Rev. Mod. Phys., 94, Oct-Dec 2022



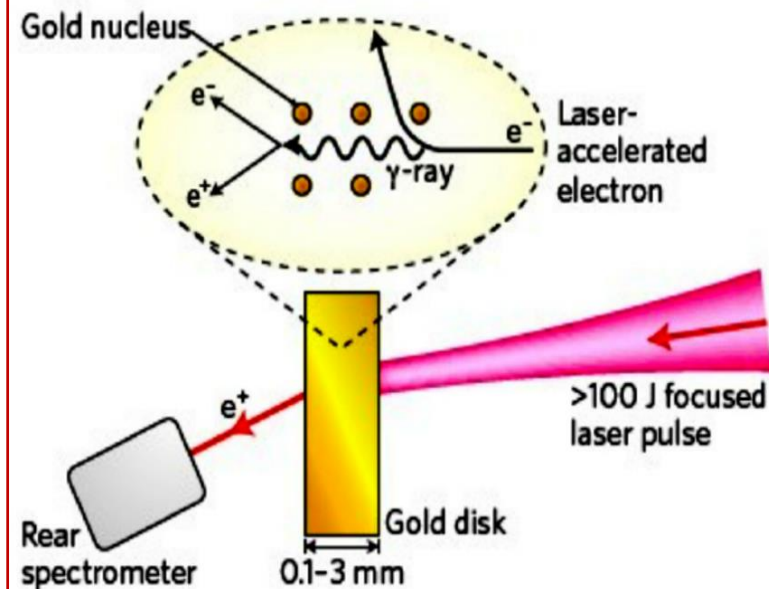
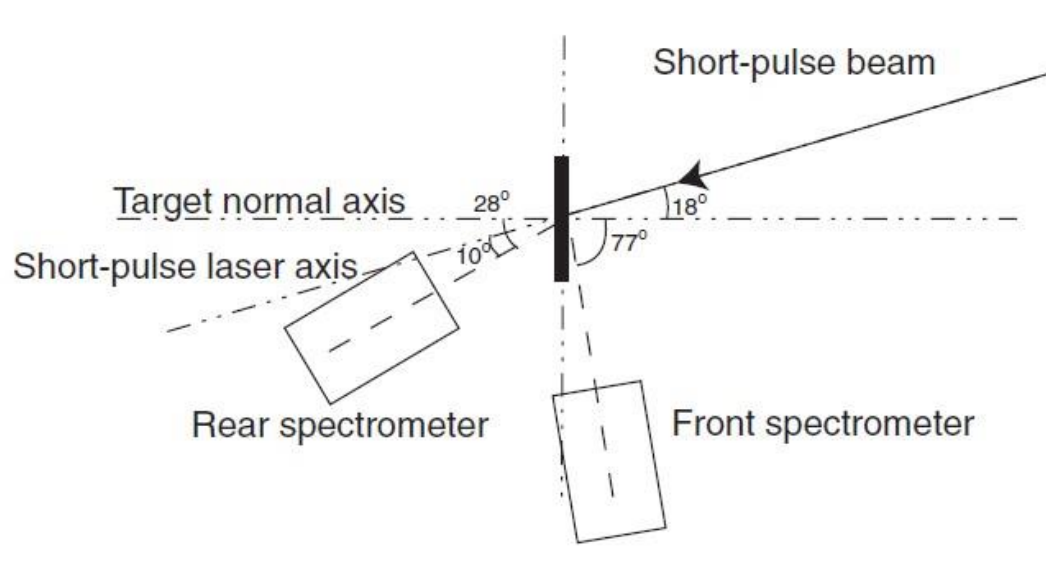
Multiphoton Breit-Wheeler Process:
 $\gamma + n \gamma_L \rightarrow e^+ e^-$



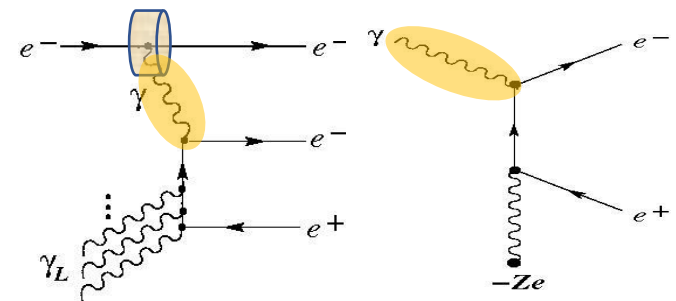
4. Competitive projects: National Ignition Facility

So far, relatively simple experimental works have been done.

Hui Chen et al. in “*Relativistic Positron Creation Using Ultraintense Short Pulse Lasers*” [28] with the **Titan** laser, one of the two lasers in the **Jupiter facility** at the **National Ignition Facility** (USA), with an energy of 250 J, by irradiating a high-Z target (Au ~1 mm) with laser pulses of 1054 nm, duration ~1 ps, intensity ~ 1×10^{20} W/cm² (see Fig.), 2×10^{10} positrons/sr were obtained, with energy < 20 MeV, with an anisotropic angular distribution, where the number of positrons recorded in the -77° direction being 10 times higher than the one on the 28° direction from the normal on the surface of the target.



Positrons are produced predominately by the **Bethe-Heitler process** and have an effective energy of 2–4 MeV, with the distribution peaking at 4–7 MeV [28]. In this process the electrons, resulting from the interaction of the laser pulse with the target, produces bremsstrahlung gamma radiation of the order of MeV, which in turn, in the interaction with the electric field of the nucleus, generates electron-positron pairs. Such studies were further carried out with ultra-intense laser [35-41].



4. ELI-NP remarks & expectations

(LUXE remark)

Dimensionless Intensity parameter
(field energy density) ξ^2

$$\xi^2 = \left(\frac{eE_L}{m_e \omega_L} \right)^2 = \left(\frac{m_e E_L}{\omega_L E_{cr}} \right)^2 ; E_{cr} = \frac{m_e^2 c^3}{e \hbar} ; c = \hbar = 1$$

For $\xi \leq 1$ probability of net absorption of n laser photons $\propto (\xi^2)^n \sim \alpha^n$

Dimensionless Intensity quantum parameter
(quantumness) χ_e

$$\chi_e = \left(2\gamma_e \frac{\omega_L}{m_e} \right) \xi = 2\gamma_e \frac{E_L}{E_{cr}}$$

χ_e accounts of the quantum nonlinear effect in e - γ laser collision.

Ratio of the laser RMS field E_L (in the e^- rest frame) to the critical field E_{cr}

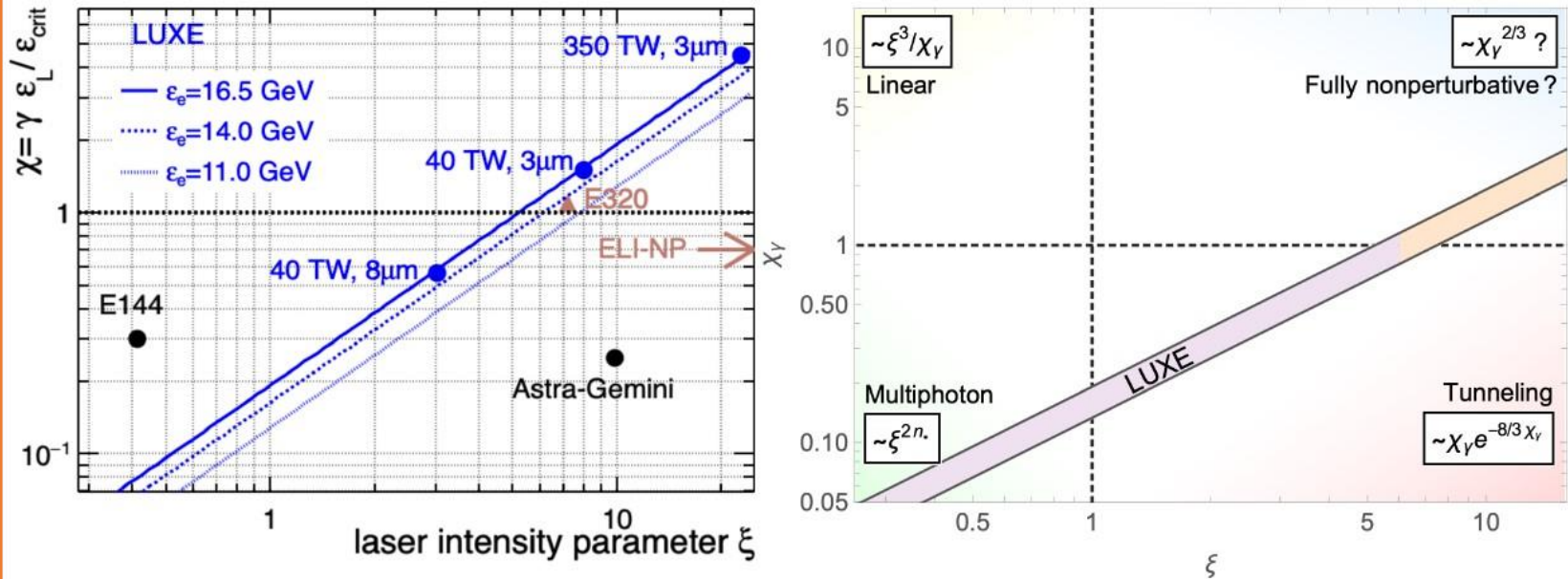
laser power to reach the Schwinger field ($\chi \sim 1$)

- non-relativistic photons : $I = 2 \cdot 10^{29}$ W/cm² (beyond currently achievable values)
- EU-XFEL: $E_\gamma \approx 10$ GeV: $I = 10^{20}$ W/cm² (well-tested laser technology)
- ELI-NP: $E_\gamma \approx 1$ GeV: $I = 10^{22}$ W/cm² (state-of-the-art laser needed)

G. Grzelak, LUXE slides, 2020

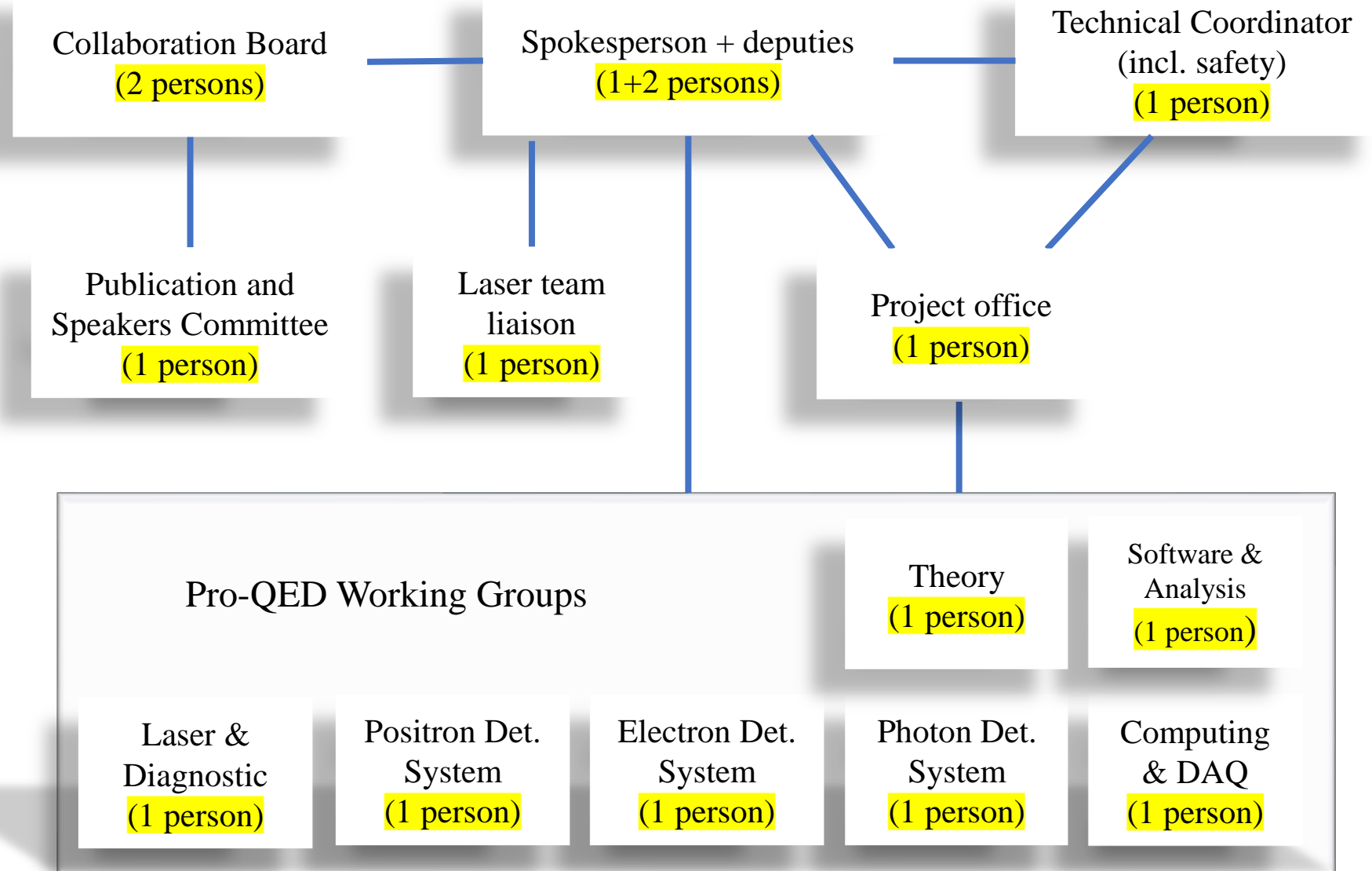
4. ELI-NP expectations – no any proposal

Strong-field QED parameter space



- E144: SLAC experiment in 1990s used 46.6 GeV electron beam.
 - ➔ Values up to $\chi \sim 0.3$, $\xi \sim 0.4$, observed $e^- + n \gamma_L \rightarrow e^- + e^+ + e^-$ and power law.
- Astra-Gemini: laser-wake field experiment in RAL with ~ 1 GeV electrons.
- E320: new experiment at SLAC.
- **ELI-NP: in the future ...**
- LUXE: to cover broad parameter space and be the first to investigate high χ and high ξ . To measure collisions of real GeV photons and laser photons.

5. Organizational Chart



5. Summary

- **Pro-QED project** - study of fundamental QED processes in an unexplored region of QED into the non-perturbative regime, possible to search at ELI-NP.
- Presented the state of the art and current results of experimental searches for particle production in light – matter interactions.
- Have intensive lectures on fundamental QED processes.
- Evaluation of the ELI-NP possibility to be used in the unexplored QED non-perturbative processes studies.
- A strong team must be prepared as to deliver a **Letter of Intent** for an experimental setup and finally the ability to **perform the experiment** leading to exciting physics results
(conditioned by an adequate funding for manpower, equipment and materials).

Thank you

References

- [1] F. Sauter, “Über das Verhalten eines Elektrons im homogenen elektrischen Feld nach der relativistischen Theorie Diracs“ Z. Phys. 69 (1931) 742;
W. Heisenberg, H. Euler, „Folgerungen aus der Diracschen Theorie des Positrons“ Z. Phys. 98 (1936) 714;
J. S. Schwinger, „On Gauge Invariance and Vacuum Polarization“, Phys. Rev. 82, 664 (1951).
- [2] G. Breit and J.A. Wheeler, “Collision of Two Light Quanta”, Phys. Rev. 46, 1087 (1934).
- [3] H.A. Bethe and W. Heitler, “On the stopping of fast particles and on the creation of positive electrons”, Proc. Roy. Soc. A146, 83 (1934).
- [3] H. R. Reiss, “Absorption of light by light”, J. Math. Phys. 3, 59 (1962).
- [4] N. B. Narozhny, A. I. Nikishov, and V. I. Ritus, “Quantum Processes in the Field of a Circularly Polarized Electromagnetic Wave”, Sov. Phys. JETP 20, 622 (1965).
- [5] V. I. Ritus, “Quantum effects of the interaction of elementary particles with an intense electromagnetic field”, J. Sov. Laser Res. 6, 497 (1985).
- [7] O.C. De Jager et al., “Estimate of the intergalactic infrared radiation field from γ -ray observations of the galaxy Mrk421”, Nature 369, 294 (1994).
- [8] O. Pike – interview “Light into matter”, Nature Photonics, Vol 8, 2014
- [9] D. B. Blaschke et al., “Influence of Laser Pulse Parameters on the Properties of e^-e^+ Plasmas Created from Vacuum”, Contrib. Plasma Phys. 53, 165 (2013).
- [10] A. I. Titov, B. Kampfer, H. Takabe, and A. Hosaka, “Breit-Wheeler process in very short electromagnetic pulses”, Phys. Rev. A 87, 042106 (2013)
- [11] G. V. Dunne, H. Gies, and R. Schutzhold, “Catalysis of Schwinger vacuum pair production”, Phys. Rev. D 80, 111301 (2009).
- [12] P. H. Bucksbaum, G. V. Dunne et al., „Understanding the Fully Non-Perturbative Strong-Field Regime of QED” SNOWMASS-2021, LoI to Theory Frontier (2020).
- [13] C. Bula et al. [E144], “Observation of nonlinear effects in Compton scattering,” Phys. Rev. Lett. 76, 3116-3119(1996)
- [14] D. Burke et al. [E144], “Positron production in multi-photon light by light scattering”, Phys. Rev. Lett. 79, 1626-1629 (1997)
- [15] M. Altarelli, R. Assmann, F. Burkart, B. Heinemann, T. Heinzl, T. Koffas, A. Maier, D. Reis, A. Ringwald and M. Wing, “Summary of strong-field QED Workshop”, arXiv:1905.00059 (2019).
- [16] H. Abramowicz et al., “Letter of Intent for the LUXE Experiment”, arXiv:1909.00860 (2019).
- [17] S. Meuren on behalf of the E-320 Collaboration, “Probing Strong-field QED at FACET-II (SLAC E-320)” (2019)
- [18] I. Turcu et al, “High field physics and QED experiments at ELI-NP”, Rom. Rep. Phys. 68, Supplement, S145 (2016).

References

- [19] R. Falcone, F. Albert, F. Beg, S. Glenzer, T. Ditmire, T. Spinka, and J. Zuegel, “*Workshop Report: Brightest Light Initiative*”, arXiv:2002.09712 (2020).
- [20] S. Baalrud, N. Ferraro, L. Garrison, N. Howard, C. Kuranz, J. Sarff, E. Scime, and W. Solomon, “*A Community Plan for Fusion Energy and Discovery Plasma Sciences – Report of the 2019–2020 American Physical Society Division of Plasma Physics Community Planning Process*”, APS-DPP-CPP, 1-186 (2020).
- [21] S. Meuren, P. H. Bucksbaum, N. J. Fisch, F. Fiúza, S. Glenzer, M. J. Hogan, K. Qu, D. A. Reis, G. White and V. Yakimenko, “*On Seminal HEDP Research Opportunities Enabled by Colocating Multi-Petawatt Laser with High-Density Electron Beams*”, arXiv:2002.10051 (2020).
- [22] V. Yakimenko, S. Meuren, F. Del Gaudio et al., “*Prospect of Studying Nonperturbative QED with Beam-Beam Collisions*”, Phys. Rev. Lett. 122, no.19, 190404 (2019).
- [23] 2019 SLAC workshop: Physics Opportunities at a Lepton Collider in the Fully Nonperturbative QED Regime.
- [23] Extremely High Intensity Laser Physics Conference: EXHILP 2019.
- [24] Greiner W. and Reinhardt J. 2008 „Quantum Electrodynamics“ (Berlin: Springer)
- [25] B Kettle et al. ”*A laser–plasma platform for photon–photon physics: the two photon Breit–Wheeler process*” *New J. Phys.* **23** 115006, (2021)
- [26] Bula C. et al, “*Observation of Nonlinear Effects in Compton Scattering*” (SLAC), Phys.Rev.Lett. 76 3116 (1996)]
- [27] Bula C. (E-144 SLAC), “*Positron Production in Multiphoton Light-by-Light Scattering*” AIP Conference Proceedings 396, 165 (1997)
- [28] Hui Chen et al., “*Relativistic Positron Creation Using Ultraintense Short Pulse Lasers*”, Phys. Rev. Lett. 102, 105001 (2009).
- [29] M. Jirka et al., “*Electron dynamics and γ and e^-e^+ production by colliding laser pulses*”, Phys. Rev. E 93, 023207 (2016).
- [30] J. M. Cole, et al., “*Experimental evidence of radiation reaction in the collision of a high-intensity laser pulse with a laser-wakefield accelerated electron beam*”, Phys. Rev. X 8, 011020 (2018).
- [31] Hartin, A. Ringwald, and N. Tapia, “*Measuring the boiling point of the vacuum of quantum electrodynamics*”, Phys. Rev D 99, 036008 (2019)
- [32] T. N. Wistisen, A. Di Piazza, H. V. Knudsen, and U. I. Uggerhøj, “*Experimental evidence of quantum radiation reaction in aligned crystals*”, Nat. Commun. 9, 795 (2018)
- [33] K. Poder et al., “*Experimental signatures of the quantum nature of radiation reaction in the field of an ultraintense laser*”, Phys. Rev. X 8, 031004 (2018).
- [34] W. Heitler, “*The Quantum Theory of Radiation*” (Clarendon Press, Oxford, 1954)]

References

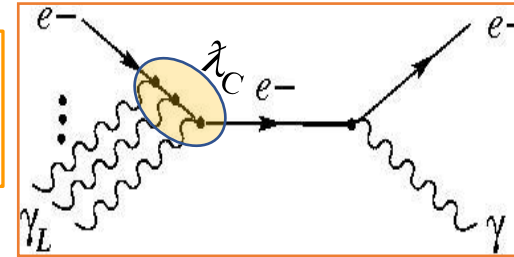
- [35] E. P. Liang, S. C. Wilks, M. Tabak, “*Pair Production by Ultraintense Lasers*”, Phys. Rev. Lett. 81, 4887 (1998).
- [36] B. Shen and J. Meyer-ter-Vehn, “*Pair and γ -photon production from a thin foil confined by two laser pulses*”, Phys. Rev. E 65, 016405 (2001).”,
- [37] P. L. Shkolnikov et al., “*Positron and gamma-photon production and nuclear reactions in cascade processes initiated by a sub-terawatt femtosecond laser*”, Appl. Phys. Lett. 71, 3471 (1997).
- [38] D. A. Gryaznykh, Y. Z. Kandiev, and V. A. Lykov, “*Estimates of electron-positron pair production in the interaction of high-power laser radiation with high-Z targets*”, JETP Lett. 67, 257 (1998).”,
- [39] V. I. Berezhiani, D. P. Garuchava, and P. K. Shukla, “*Production of electron–positron pairs by intense laser pulses in an overdense plasma*”, Phys. Lett. A 360, 624 (2007).
- [40] T. E. Cowan et al., “*High energy electrons, nuclear phenomena and heating in petawatt laser-solid experiments*” Laser and Particle Beams 17, 773 (1999).
- [41] C. Gahn et al., “*Generating positrons with femtosecond-laser pulses*”, Appl. Phys. Lett. 77, 2662 (2000)
- [42] I. C. E. Turcu et al., “*Quantum electrodynamics experiments with colliding petawatt laser pulses*”, High Power Laser Science and Engineering, (2019), Vol. 7, <https://doi.org/10.1017/hpl.2018.66>
- [43] F. Negoita, et al. “*Laser Driven Nuclear physics at ELI-NP*”, Rom. Rep. Phys. 68, S37 (2016).
- [44] S. Gales, et al., “*The extreme light infrastructure-nuclear physics (ELI-NP) facility: new horizons in physics with 10 PW ultra-intense lasers and 20 MeV brilliant gamma beams*”, Rep. Prog. Phys. 81, 094301 (2018)
- [45] J. Wardle et al., “*Electron–positron jets associated with the quasar 3C279*”, Nature (London) 395, 457 (1998).
- [46] P. Meszaros, “*Theories of Gamma-Ray Bursts*”, Annual Rev. Astron. Astrophys. 40, 137 (2002).
- [47] H. A. Weldon, “*Measuring T_c of the quark-gluon plasma with e^+e^- pairs*”. Phys. Rev. Lett. 66, 293 (1991).
- [48] E. G. Blackman and G. B. Field, “*Ohm’s law for a relativistic pair plasma*”, Phys. Rev. Lett. 71, 3481 (1993).
- [49] A. Gonoskov, T. G. Blackburn, and M. Marklund, “*Charged particle motion and radiation in strong electromagnetic fields*”, Rev. Mod. Phys., 94. 045001 (Oct–Dec 2022).
- [50] Kun Xue et al, “*Generation of arbitrarily polarized GeV lepton beams via nonlinear Breit-Wheeler process*”, Fundamental Research 2 (2022) 539-545
- [51] Y. I. Salamin, S.X. Hu, K.Z. Hatsagortsyana, C.H. Keitel, “*Relativistic high-power laser–matter interactions*”, Phys. Rep. 427 (2006) 41
- [52] D.L. Burke et al., “*Positron Production in Multiphoton Light-by-Light Scattering*” Phys. Rev. Lett. 79 (1997) 1626.
- [53] C. Bamber et al., “*Studies of nonlinear QED in collisions of 46.6 GeV electrons with intense laser pulses*”, Phys. Rev. D 60 (1999) 092004.

Classical non-linearity parameter ξ (field energy density)

Charge-field coupling parameter - ξ

ξ - number of γ_L laser photons interacting on λ_C (the reduced Compton wave length for the e^+e^- production range by vacuum fluctuations):

Laser electric field:
 $E_L \equiv E_{rms}$



$$\xi = eE_L \frac{\lambda_C}{\hbar\omega_L} = \frac{eE_L}{m_e c \omega_L}$$

Transfer energy to electron from EL field over λ_C = where $\lambda_C = \frac{\hbar}{m_e c}$
 = energy of the laser photon
 = initial nr. of laser photons γ_L

$$\xi = \frac{eE_L}{\hbar\omega_L} \frac{\hbar}{m_e c} = \frac{E_L}{\hbar\omega_L} \frac{\hbar e}{m_e^2 c^3} m_e c^2 \equiv \frac{m_e c^2}{\hbar\omega_L} \frac{E_L}{E_{cr}}$$

$$E_{cr} = \frac{m_e^2 c^3}{\hbar e}$$

$$\xi \sim \frac{E_L}{E_{cr}} = \sqrt{\frac{I}{I_{cr}}}$$

Intensity parameter

The same parameter, but expressed as

$$a = \frac{eE_L}{m_e c \omega_L} = \frac{eE_L}{m_e c} \frac{\lambda_L}{2\pi c} \quad \text{where} \quad \omega_L = 2\pi\nu_L = 2\pi \frac{c}{\lambda_L}$$

ξ^2 - photon density of the laser beam

When ξ is small the most probable are the processes with minimum possible number of photons.

At $\xi \ll 1$ the probabilities equals the perturbation (linear) theory probabilities and plane waves play a role of an individual photon.

At $\xi \sim 1$ or $\xi > 1$ the probabilities of absorbing different number of photons become comparable and the process becomes multiphoton, i.e., the probability has an essentially nonperturbative (nonlinear) dependence on the field.

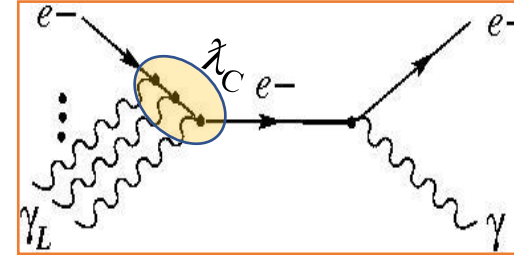
Thus ξ is the classical nonlinearity parameter.

$\xi \gg 1$ with modern laser technology. The EM pulse with highest reported intensity had $\xi \approx 102$.

Quantum non-linearity parameter χ_e

ξ – defined in photon energy units: $\xi = eE_L \frac{\lambda_c}{\hbar\omega_L}$

χ_e – defined in electron mass units: $\chi \sim eE_L \frac{\lambda_c}{m_e c^2}$



The Classical non-linearity parameter ξ (relative to the energy transferred from the field)

$$\xi = eE_L \frac{\lambda_c}{\hbar\omega_L} = \frac{m_e c^2}{\hbar\omega_L} \frac{E_L}{E_{cr}}$$

where $\lambda_c = \frac{\hbar}{m_e c}$ $E_{cr} = \frac{m_e^2 c^3}{\hbar e}$

Quantum non-linearity parameter χ_e (relative to the electron energy) $\gamma_e = \frac{\mathcal{E}_e}{m_e c^2} = \frac{e^- \text{ energy}}{e^- \text{ rest energy}}$

$$\chi_e = \frac{\mathcal{E}_e}{m_e c^2} \frac{E_L}{E_{cr}} = \gamma_e \frac{E_L}{E_{cr}} = \frac{E^*}{E_{cr}}$$

Ratio of the laser RMS field E_L (in the e^- rest frame) E^* to the critical field E_{cr}

$$\chi_e = \gamma_e \frac{E_L}{E_{cr}} = \left(\gamma_e \frac{\hbar\omega_L}{m_e c^2} \right) \xi$$

Dimensionless quantum parameter (quantumness)

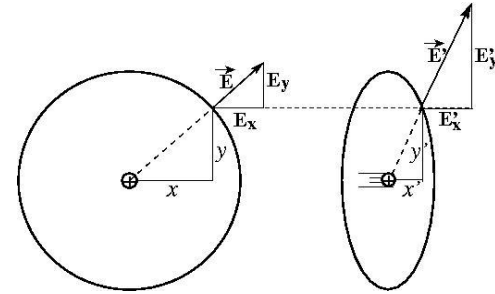
χ_e accounts of the quantum nonlinear effect in $e^- \gamma$ laser collision

Electric Field Boost

In the moving electron reference system, the field E_L is $\gamma_e = \mathcal{E}_e/m_e c^2$ times larger than in the rest system: $E^* = \gamma_e E_L$

For example, for $\mathcal{E}_e = 1 \text{ GeV}$; $\gamma_e = 10^3 \text{ MeV}/0.5 \text{ MeV} = 2 \cdot 10^3$ and also the electron “sees” a boosted laser field $E^* = \gamma_e E_L$ in its own rest frame.

If $\gamma_e E_L > E_{cr}$ it interacts with laser photons and extract the e^+e^- pair, just like a GeV γ photon interacts with laser photons.



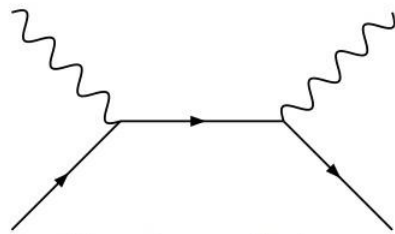
When a laser field of strength E_L is viewed in the rest frame of a relativistic, counter-propagating particle with laboratory energy \mathcal{E}_e and Lorentz factor $\gamma_e = \mathcal{E}_e/mc^2 \gg 1$ the laser field E_L is boosted to $E^* = \gamma_e E_L$.

For $\mathcal{E}_e = 46.6 \text{ GeV}$ electron has $\gamma_e = 9 \times 10^4$ so if it collides head on with a 527-nm laser pulse of strength $\xi = 1$ the field in the electron's rest frame is $E^* = 1.1 \times 10^{18} \text{ V/m}$.

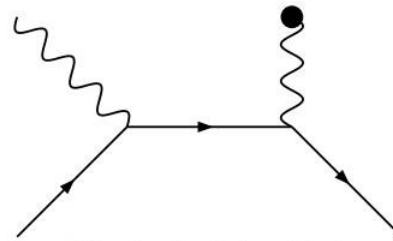
This is close to the QED critical field strength $E_{cr} = m^2 c^3 / eh = 1.3 \times 10^{18} \text{ V/m}$ at which the energy gain of an electron accelerating over a Compton wavelength is its rest energy, and at which a static electric field would spontaneously break down into electron-positron pairs.

2. Goal of the Project

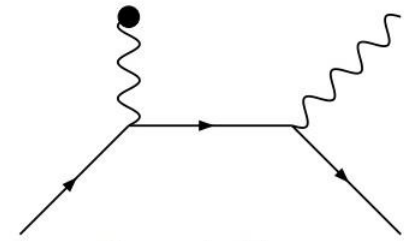
Study of the simplest QED interaction processes between light and matter possible to be measured at ELI-NP Facility. Special attention to pair production in photon – nucleus interaction (Bethe-Heitler).



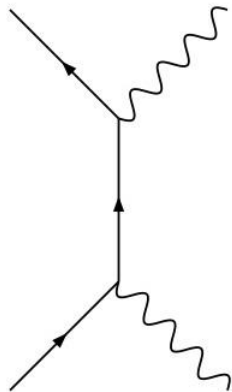
Compton scattering



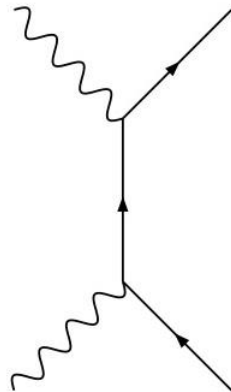
Photoelectric effect



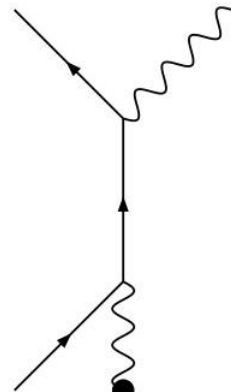
Bremsstrahlung



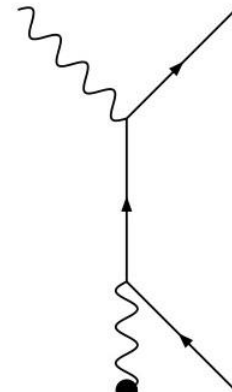
Dirac annihilation



Breit-Wheeler pair production

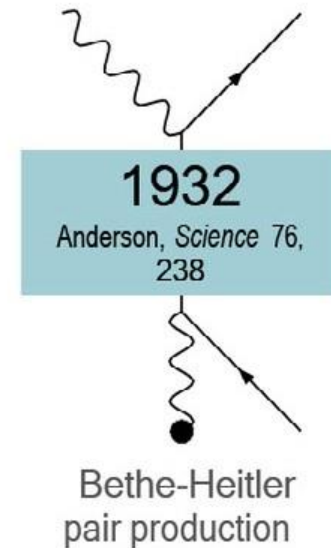
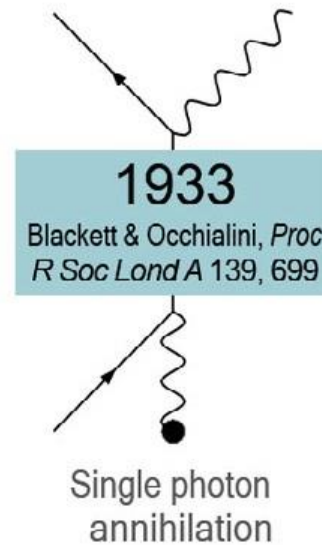
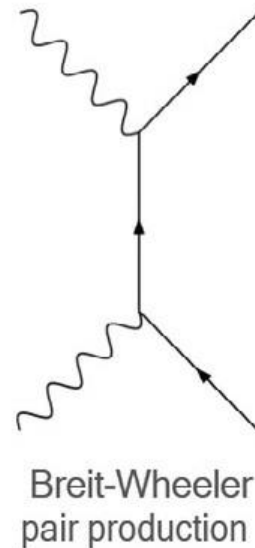
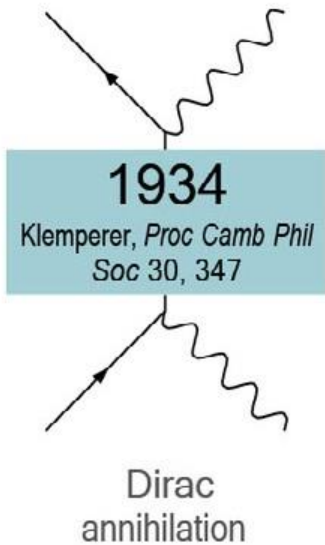
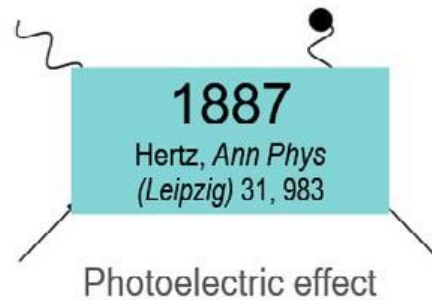
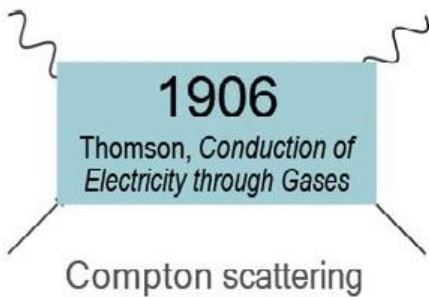


Single photon annihilation

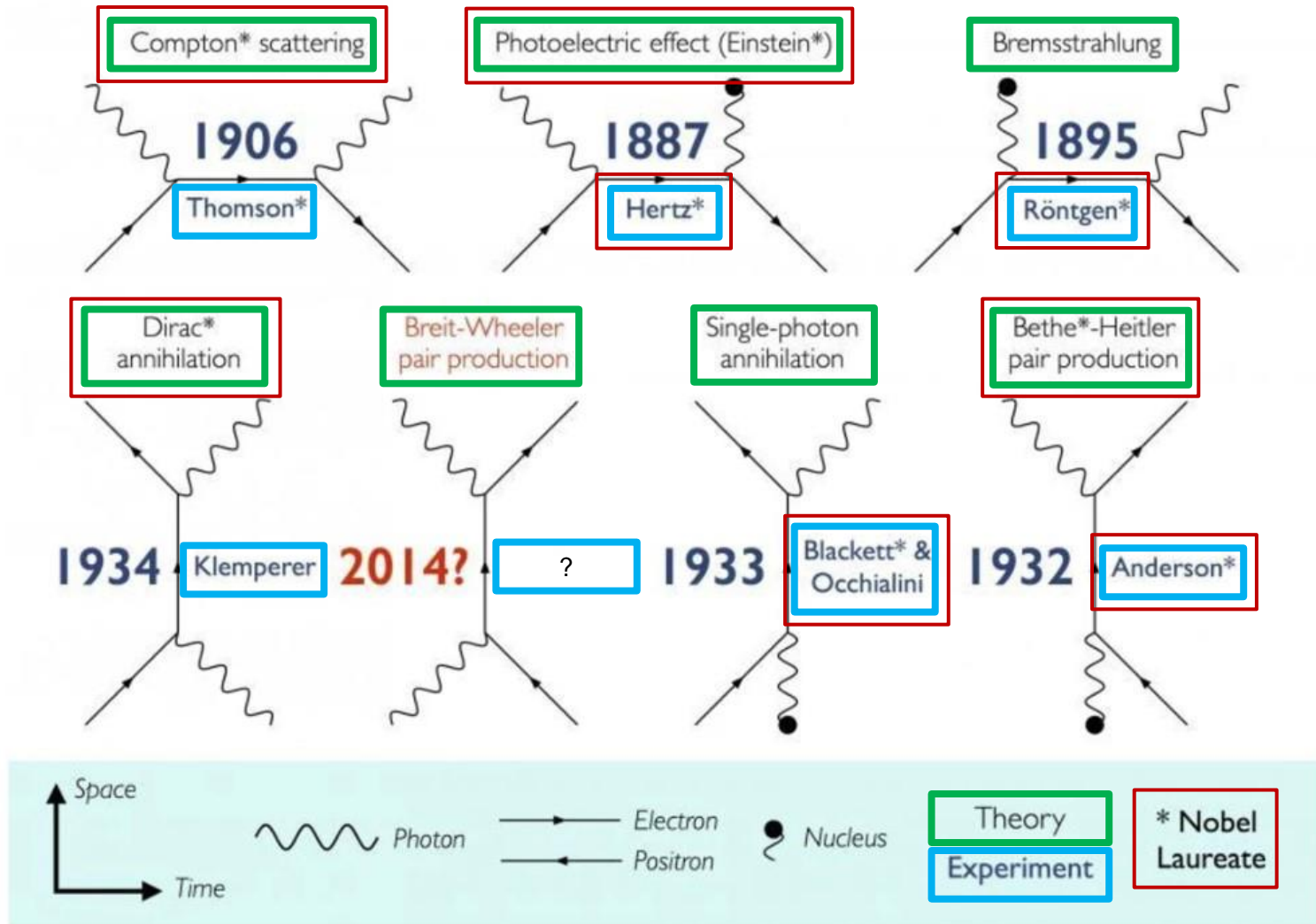


Bethe-Heitler pair production

The simplest interactions between light and matter: earliest results of QED



1. Light – Matter interaction processes



— This chart shows Feynman diagrams that describe the interaction of matter and light. Breit-Wheeler pair production has not yet been demonstrated experimentally.

PROBING NONLINEAR VACUUM

It was shown in a number of papers that the e^+e^- pair production can be observed in an EM field, which is a superposition of two colliding EM pulses [17, 18]. In the antinodes of an emerging standing light wave the invariant electric field, which is responsible for pair production, acquires its maximum value. The estimates show that for **tightly focused laser pulses** the intensity of 2.5×10^{26} W/cm² is needed to observe pair production, which is three orders of magnitude less than the intensity corresponding to the "critical" field strength [18].

PRINCIPAL EXPERIMENTAL SCHEMES

There are two principle experimental schemes aimed at the study of particle physics effects at high laser intensity:

- (i) colliding laser pulses (all optical setup) and
- (ii) laser - e-beam interaction (See Figure 2).

The first one could be employed for the study of direct vacuum breakdown, *i.e.*, the e^+e^- pair production under the action of intense EM field and the subsequent "avalanche".

The second scheme will allow for the study of basic processes: photon emission by an electron and a photon conversion into an electron-positron pair in intense EM field.

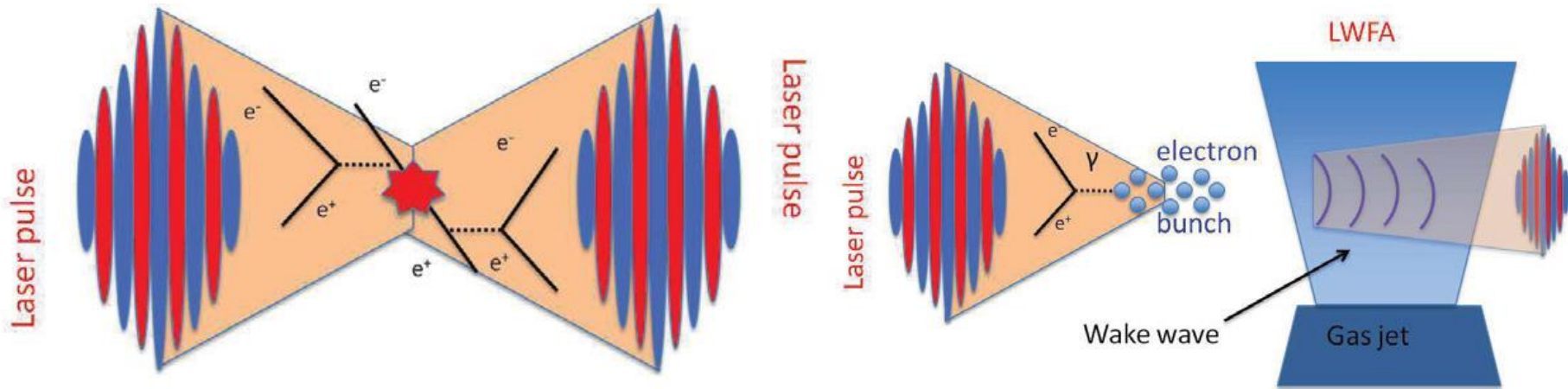
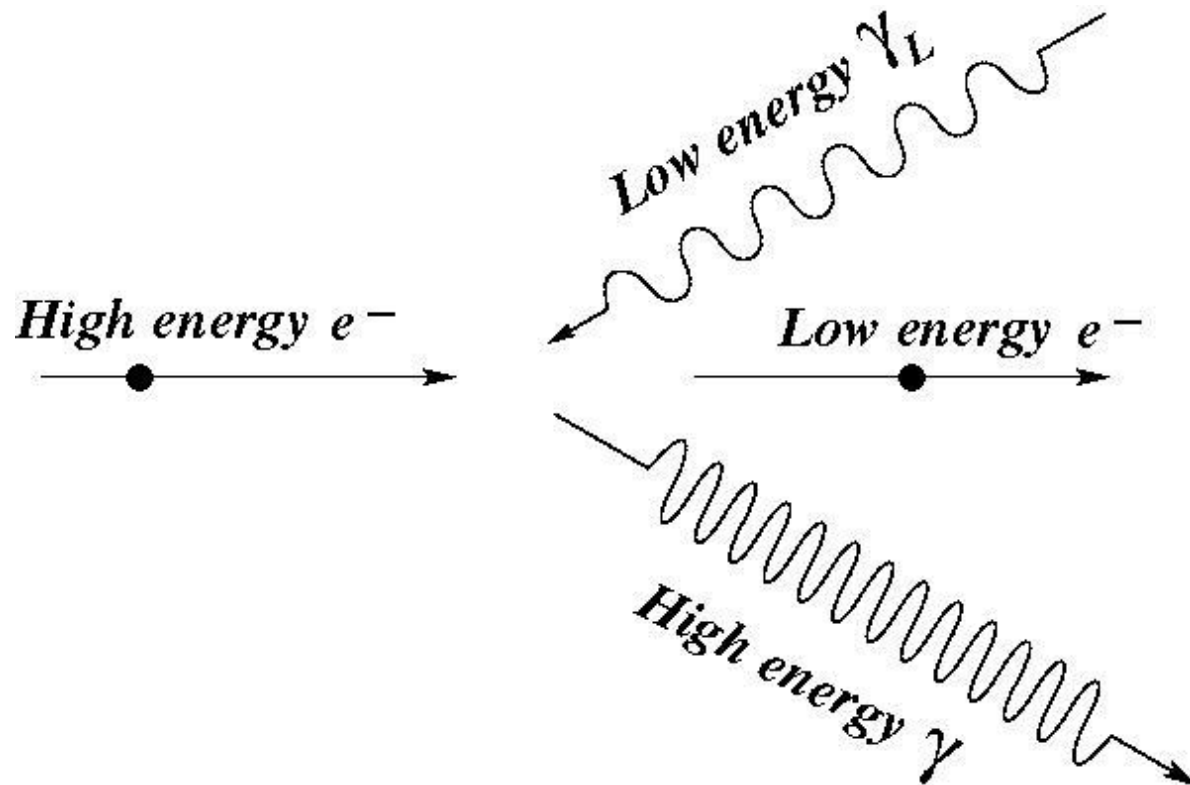
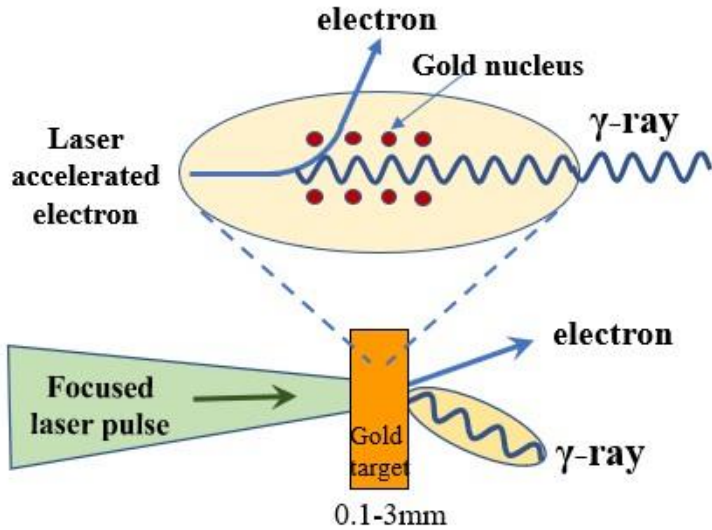


FIGURE 2. Principle experimental schemes aimed at the study of (i) colliding laser pulses (all optical setup); (ii) laser - e-beam interaction.

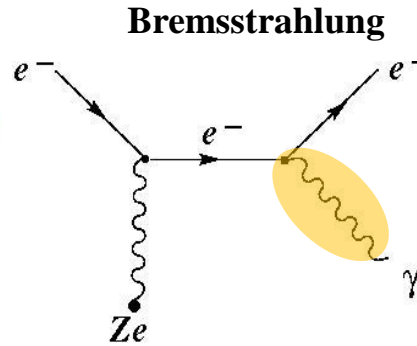


2. Particular interest - multiphoton Bethe-Heitler pair production

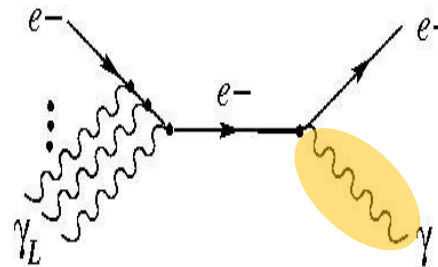
Wakefield electron acceleration



MeV γ sources

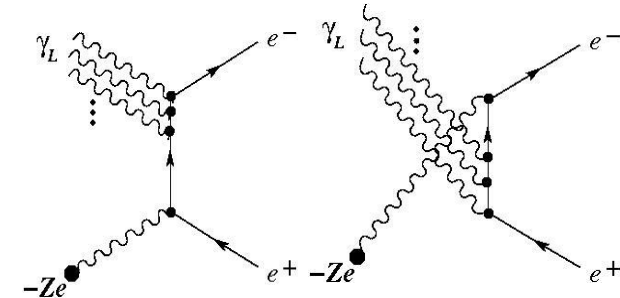
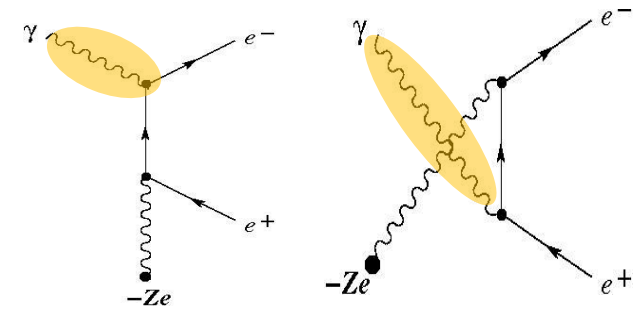


Inverse Compton scattering



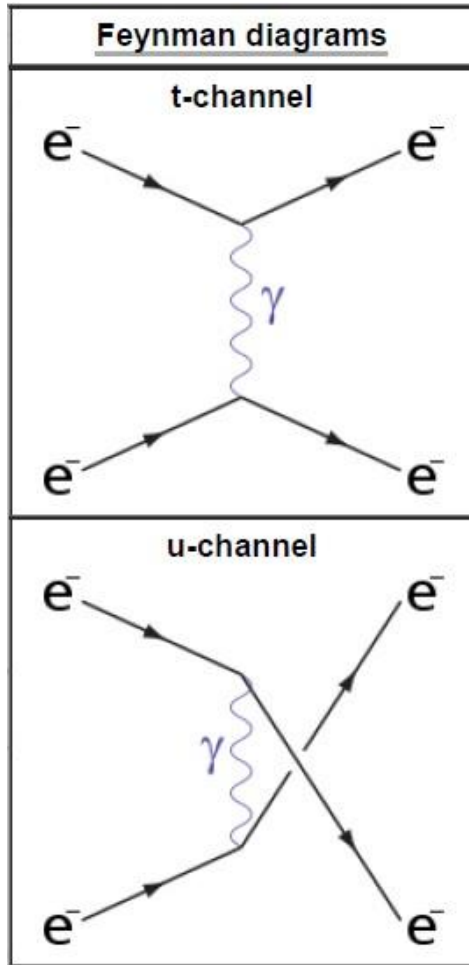
Pair production

Bethe-Heitler pair production



Bethe-Heitler pair production by laser beam interaction with nuclei - special interest for ELI-NP

Feynman Diagram - Moller Scattering



$$d\sigma = \frac{|\mathcal{M}|^2}{F} dLips$$

$$i\mathcal{M}_t = (-ie)^2 \bar{u}(p_3) \gamma^\mu u(p_1) \frac{-i}{t} \bar{u}(p_4) \gamma_\mu u(p_2)$$

$$i\mathcal{M}_u = (-ie)^2 \bar{u}(p_3) \gamma^\mu u(p_2) \frac{-i}{u} \bar{u}(p_4) \gamma_\mu u(p_1)$$

$$i\mathcal{M} = i(\mathcal{M}_t - \mathcal{M}_u)$$

$$= -i(-ie)^2 \left[\frac{1}{t} \bar{u}(p_3) \gamma^\mu u(p_1) \bar{u}(p_4) \gamma_\mu u(p_2) - \frac{1}{u} \bar{u}(p_3) \gamma^\mu u(p_2) \bar{u}(p_4) \gamma_\mu u(p_1) \right]$$

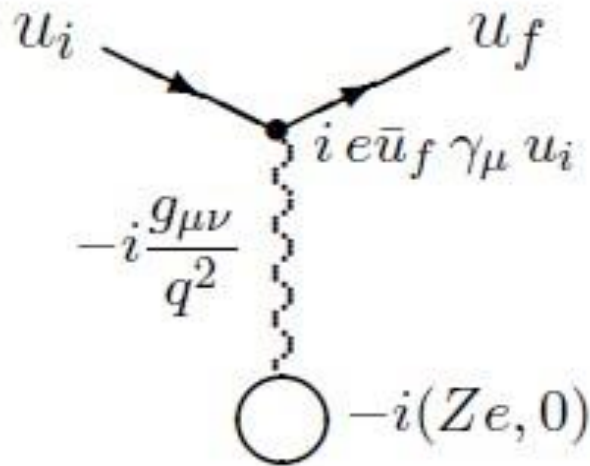
$$p_1 = (E, 0, 0, p), \quad p_2 = (E, 0, 0, -p)$$

$$p_3 = (E, p \sin \theta, 0, p \cos \theta), \quad p_4 = (E, -p \sin \theta, 0, -p \cos \theta)$$

$$\begin{aligned} \overline{|\mathcal{M}|^2} &\equiv \frac{1}{4} \sum_{\text{spins}} |\mathcal{M}|^2 \\ &= 2e^4 \left\{ \frac{1}{t^2} (s^2 + u^2 - 8m^2(s+u) + 24m^4) \right. \\ &\quad + \frac{1}{u^2} (s^2 + t^2 - 8m^2(s+t) + 24m^4) \\ &\quad \left. + \frac{2}{tu} (s^2 - 8m^2s + 12m^4) \right\} \end{aligned}$$

$$\frac{d\sigma}{d\Omega} = \frac{\alpha^2}{E_{CM}^2 p^4 \sin^4 \theta} \left[4(m^2 + 2p^2)^2 + (4p^4 - 3(m^2 + 2p^2)^2) \sin^2 \theta + p^4 \sin^4 \theta \right]$$

3. Feynman diagrams evaluation (example - Coulomb Scattering)



$$-i\mathcal{M} = \left(i e \bar{u}_f \gamma_0 u_i \right) \left(\frac{-i}{q^2} \right) \left(-i Z e \right)$$

$$\begin{aligned} q^2 &= (p_f - p_i)^2 = 2m^2 - 2p_i \cdot p_f = 2m^2 - 2(E_i E_f - \vec{p}_i \cdot \vec{p}_f) \\ &= 2m^2 - 2E_i E_f + 2|\vec{p}_i| |\vec{p}_f| \cos \theta = 2(m^2 - E^2) + 2|\vec{p}|^2 \cos \theta \\ &= -2|\vec{p}|^2(1 - \cos \theta) = -4|\vec{p}|^2 \sin^2(\theta/2) \end{aligned}$$

$$d\sigma = \frac{|\mathcal{M}|^2}{F} dLips$$

$$\frac{d\sigma}{d\Omega} \sim |\mathcal{M}|^2 \sim \frac{1}{\sin^4(\theta/2)}$$

(Turcu, p. 22)

The electromagnetic fields in the laser focus will be so strong that very nonlinear quantum electrodynamics (QED) effects, not yet seen in the laboratory, will play a critical role.

These nonlinear QED processes become important when the electric field in the electron's rest frame (E_{RF}) approaches the critical field for QED (the Schwinger field $E_S = 1.3 \times 10^{18} \text{ Vm}^{-1}$) [52].

I. Here we propose studying these effects in the collision of an electron bunch (energy $\gamma m_e c^2$) with an intense laser pulse (peak intensity I). In this case the quantum parameter is given by

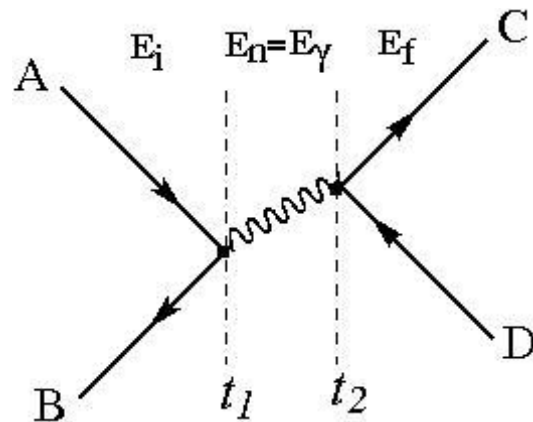
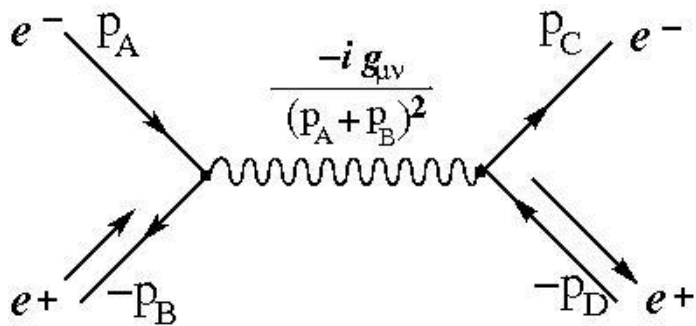
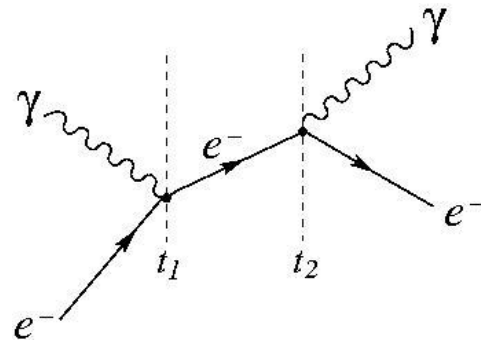
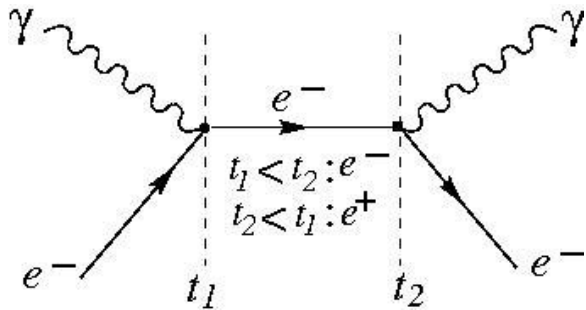
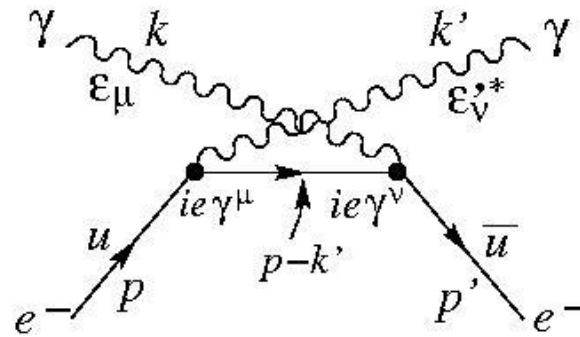
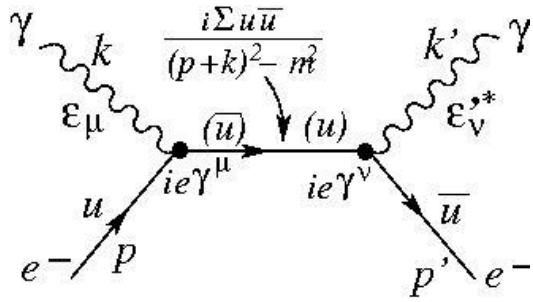
$$\eta = E_{RF}/E_S \sim (\gamma m_e c^2 / 1 \text{ GeV})(I / 10^{22} \text{ W cm}^{-2})^{1/2} \quad (10)$$

Experiments of this type using high energy electron beams produced by particle accelerators have probed the weakly non-linear strong field QED regime (SLAC [53]).

II. Recently, all-optical equivalents been performed where the electron beam was produced by laser wakefield acceleration [54–56].

These have the potential to probe the extremely non-linear $\eta \sim 1$ strong field QED regime but the necessary parameters for reaching this regime, namely $\gamma m_e c^2 > 1 \text{ GeV}$, $I \sim 10^{22} \text{ Wcm}^{-2}$ cannot be achieved simultaneously and reliably on current PW laser facilities.

ELI-NP will be able to reach these parameters and thus will enable the first exploration of several fundamental strong-field QED processes: (i) very nonlinear inverse Compton scattering and the resulting radiation reaction; (ii) very nonlinear Breit-Wheeler pair production; (iii) nonlinear Bethe-Heitler pair production



Electromagnetic spectrum

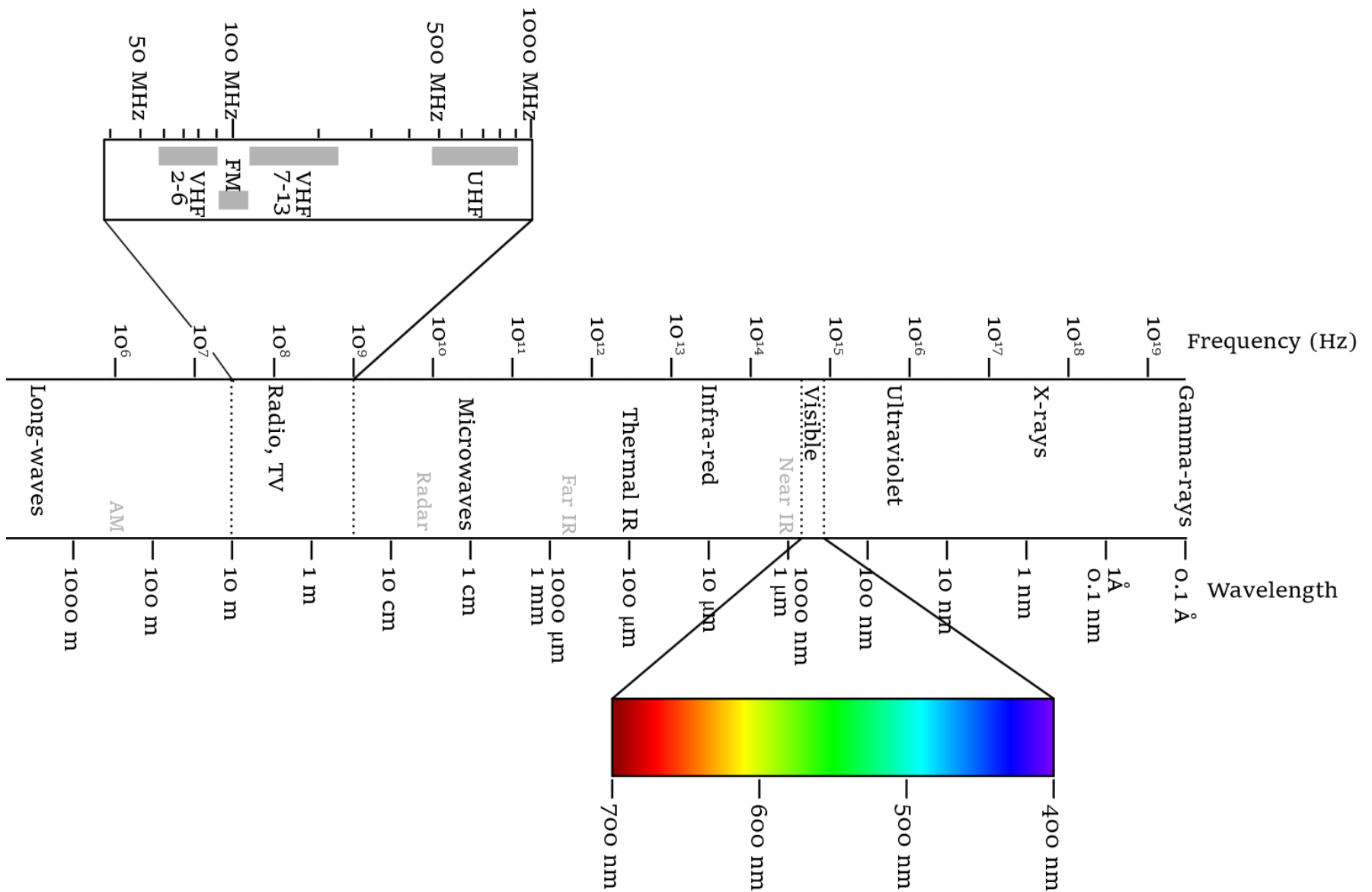


TABLE II. Parameters of the laser facilities shown in Fig. 2.

Name	Facility	Country	Wavelength (μm)	Energy (J)	Duration (fs)	Power (PW)
Station of Extreme Light	SIOM	China	0.9	1500	15	100
EP-OPAL	LLE	USA	0.8	500	20	25
SULF	SIOM	China	0.8	220	21	10
Apollon (F1)	LULI	France	0.82	150	15	10
PEARL-X	IAP	Russia	0.527	200	20	10
L4	ELI-Beamlines	Czechia	1.057	1500	150	10
HPLS	ELI-NP	Romania	0.814	200	20	10
J-EPOCH	ILE + QST	Japan	0.8	200	20	10
SULF (current)	SIOM	China	0.8	130	24	5.4
SG-II 5 PW	SIOM	China	0.808	150	30	5
CAEP-PW	CAEP	China	0.8	91	19	4.8
CoReLS	IBS	South Korea	0.8	83	20	4.15
ZEUS	CUOS	USA	0.8	60	20	3
ATLAS-3000	CALA	Germany	0.8	60	25	2.4
Qiangguang	SIOM	China	0.8	52	26	2
SG-II 5 PW	SIOM	China	0.808	37	21	1.8
Apollon	LULI	France	0.82	38	22	1.7
Nova Petawatt	LLNL	USA	1.054	660	440	1.5
BELLA	LBNL	USA	0.8	40	30	1.3
LFEX	GEKKO XII	Japan	1.054	2000	1500	1.3
J-KAREN-P	KPSI	Japan	0.82	40	30	1.3
PETAL	CEA	France	1.053	850	700	1.2
Xtreme Light III	NLCM	China	0.8	32	28	1.1
CoReLS	IBS	South Korea	0.8	33	30	1.1
Z-Petawatt	Sandia	USA	1.054	500	500	1
Vulcan Petawatt	CLF, RAL	UK	1.054	500	500	1
Orion	AWE	UK	1.053	500	500	1
Apollon (F2)	LULI	France	0.82	15	15	1
PEneLOPE	HZDR	Germany	1.03	150	150	1
VEGA-3	CLPU	Spain	0.8	30	30	1
CETAL	INFLPR	Romania	0.8	25	25	1
L2	ELI-Beamlines	Czechia	0.82	15	15	1
L3 (HAPLS)	ELI-Beamlines	Czechia	0.82	30	30	1
SG-II UP (Shenguang II)	SIOM	China	1.054	1000	1000	1
PWM (Petawatt Module)	GEKKO XII	Japan	1.054	420	470	0.89
Texas Petawatt	Univ. of Texas at Austin	USA	1.057	120	140	0.86
J-KAREN	KPSI	Japan	0.8	28	33	0.85
Xingguang-III (fs beam)	LFRC	China	0.8	20	27	0.74
OMEGA-EP (short pulse)	LLE	USA	1.053	500	700	0.71
Diocles	ELL	USA	0.8	20	30	0.67
NIF	LLNL	USA	0.3516	1.80×10^6	3.00×10^6	0.6
PEARL	IAP	Russia	0.91	24	45	0.53

TABLE II. (Continued)

Name	Facility	Country	Wavelength (μm)	Energy (J)	Duration (fs)	Power (PW)
HERCULES	CUOS	USA	0.8	15	30	0.5
Gemini	CLF	UK	0.8	15	30	0.5
Laser Megajoule	CEA	France	0.351	1.50×10^6	3.00×10^6	0.5
PHELIX	HI GSI	Germany	1.054	200	400	0.5
Titan (west)	LLNL	USA	1.053	300	700	0.43
SCAPA	Univ. of Strathclyde	UK	0.8	8.75	25	0.35
Scarlet	Ohio State Univ.	USA	0.8	10	30	0.33
Jeti200	HI Jena	Germany	0.8	4	17	0.24
ALEPH	Colorado State Univ.	USA	0.4	10	45	0.2
POLARIS	HI Jena	Germany	1.03	17	98	0.17
Arcturus	Heinrich-Heine Univ.	Germany	0.8	3.5	30	0.12
DRACO	HZDR	Germany	0.8	3.5	30	0.12

Today experiments on radiation emission and pair creation in the strong-field regime form part of the planned experimental programs at almost every major petawatt or multi petawatt laser facility, including the

- Extreme Light Infrastructure (ELI) (Weber et al., 2017; Gales et al., 2018),
- Apollon (Papadopoulos et al., 2016),
- Station of Extreme Light (Cartlidge, 2018),
- Center for Relativistic Laser Science (CoReLS) (Yoon et al., 2021),
- J-KAREN-P (Kiryama et al., 2020),
- Omega Laser Facility (Bromage et al., 2019),
- Zetawatt-Equivalent Ultrashort Pulse Laser System (ZEUS) (Nees et al., 2020),
- conventional accelerator facilities (Abramowicz et al., 2019; Meuren, 2019).

(A. Gonoskov, T. G. Blackburn, and M. Marklund, S. S. Bulanov, **REVIEWS OF MODERN PHYSICS, VOLUME 94, OCTOBER–DECEMBER 2022.**)